Atmos. Chem. Phys., 12, 5163–5187, 2012
www.atmos-chem-phys.net/12/5163/2012/
doi:10.5194/acp-12-5163-2012

Atmospheric Chemistry and Physics

Airborne measurements of trace gases and aerosols over the London metropolitan region

G. R. McMeeking[1,*], M. Bart[2,], P. Chazette[3], J. M. Haywood[4,5], J. R. Hopkins[6], J. B. McQuaid[2], W. T. Morgan[1], J.-C. Raut[7], C. L. Ryder[8], N. Savage[4], K. Turnbull[4], and H. Coe[1]**

[1]Centre for Atmospheric Science, University of Manchester, Manchester, UK
[2]School of Earth and Environment, University of Leeds, Leeds, UK
[3]Laboratoire des Sciences du Climat et de l'Environnement, Laboratoire mixte CEA-CNRS-UVSQ, CEA Saclay, Gif-sur-Yvette, France
[4]Observation Based Research, Met Office, Exeter, UK
[5]College of Engineering, Mathematics and Physical Sciences, University of Exeter, Exeter, UK
[6]Department of Chemistry, University of York, York, UK
[7]Laboratoire Atmosphères, Milieux et Observations Spatiales, Laboratoire mixte CNRS-UVSQ-UPMC, Université Paris, Paris, France
[8]Department of Meteorology, University of Reading, Reading, UK
[*]now at: Department of Atmospheric Science, Colorado State University, Fort Collins, CO, USA
[**]now at: Aeroqual, 109 Valley Road, Auckland 1024, New Zealand

Correspondence to: G. R. McMeeking (gavin@atmos.colostate.edu)

Received: 21 October 2011 – Published in Atmos. Chem. Phys. Discuss.: 16 November 2011
Revised: 9 April 2012 – Accepted: 9 May 2012 – Published: 13 June 2012

Abstract. The Emissions around the M25 motorway (EM25) campaign took place over the megacity of London in the United Kingdom in June 2009 with the aim of characterising trace gas and aerosol composition and properties entering and emitted from the urban region. It featured two mobile platforms, the UK BAe-146 Facility for Airborne Atmospheric Measurements (FAAM) research aircraft and a ground-based mobile lidar van, both travelling in circuits around London, roughly following the path of the M25 motorway circling the city. We present an overview of findings from the project, which took place during typical UK summertime pollution conditions. Emission ratios of volatile organic compounds (VOCs) to acetylene and carbon monoxide emitted from the London region were consistent with measurements in and downwind of other large urban areas and indicated traffic and associated fuel evaporation were major sources. Sub-micron aerosol composition was dominated by secondary species including sulphate (24 % of sub-micron mass in the London plume and 29 % in the non-plume regional aerosol), nitrate (24 % plume; 20 % regional) and organic aerosol (29 % plume; 31 % regional). The primary sub-micron aerosol emissions from London were minor compared to the larger regional background, with only limited increases in aerosol mass in the urban plume compared to the background (∼12 % mass increase on average). Black carbon mass was the major exception and more than doubled in the urban plume, leading to a decrease in the single scattering albedo from 0.91 in the regional aerosol to 0.86 in the London plume, on average. Our observations indicated that regional aerosol plays a major role on aerosol concentrations around London, at least during typical summertime conditions, meaning future efforts to reduce PM levels in London must account for regional as well as local aerosol sources.

1 Introduction

The greater London urban region is home to approximately 8–12 million people, making it the largest conurbation in the United Kingdom and one of a growing number of megacities throughout the world. Globally, over half of the world's human population lives in urban areas, many of them

megacities, and these numbers are expected to grow in the coming years. Megacities frequently have very high concentrations of observed air pollutants (Banta et al., 2005), which combined with their large populations results in serious health and visibility impacts (Garland et al., 2008; Parekh, 2001). In addition to local impacts, the large emissions of pollutants from megacities make them important contributors to air pollution on regional and global scales (Lawrence et al., 2007; Molina and Molina, 2004). Cities emit primary aerosols as well as oxides of nitrogen (NO_x) and volatile organic compounds (VOCs) that drive photochemical smog formation and also oxidise to secondary aerosol precursors.

The importance of megacity emissions has motivated several recent studies featuring a combination of measurements and numerical modelling to examine aerosol and trace gas emissions and atmospheric processing. These include the MILAGRO (Megacity Initiative: Local and Global Research Observations) (Molina et al., 2010) Mexico City case study in 2006 and the CalNex (Research at the Nexus of Air Quality and Climate Change) intensive measurement period in Los Angeles in 2010. In Europe, components of the MEGAPOLI (Megacities: Emissions, urban, regional and Global Atmospheric POLlution and climate effects, and Integrated tools for assessment and mitigation) project examined emissions from Paris, France in 2009 and 2010. It followed the original experiments conducted within the frame of the Etude et Simulation de la Qualité de l'air en region Ile-de-France (ESQUIF) program (Chazette et al., 2005; Menut et al., 2000). Results from these recent campaigns have underscored the importance of oxygenated organic and secondary inorganic aerosol species to PM concentrations even in major urban locations (e.g., Aiken et al., 2009).

In London, the introduction of air quality control strategies going back to at least the early 1990s has led to reductions in gas- and particle-phase pollutants (Bigi and Harrison, 2010). Some species, including ozone (Bigi and Harrison, 2010), have increased, while recent trends in $PM_{2.5}$ and PM_{10} (particulate matter with aerodynamic diameters $<2.5\,\mu m$ and $10\,\mu m$, respectively) concentrations have remained flat or even increased, despite predicted reductions from emissions inventories (Fuller and Green, 2006). Further reductions in PM have proved elusive. For example, the contribution from road transport was expected to decrease following the introduction of a number of control strategies, including the inner London congestion charge scheme, however the impacts of the scheme and other control strategies on surface pollutant concentrations have been mixed (Atkinson et al., 2009). The upcoming 2012 London Olympics has also drawn more attention to air quality in the London region and its potential effects on the games.

Previous measurements have provided valuable information regarding the chemical make-up and sources of PM in London, but did not provide a characterisation of background aerosol upwind of London nor described how London emissions affect aerosol properties downwind of the city. Additional measurements of aerosol chemical composition in London are needed to improve both our understanding of current trends in monitoring observations and to improve emission inventories. Better understanding of the contributions from nitrate, sulphate and secondary organic aerosol (SOA) to regional background aerosol concentrations is also needed. Motivated by these needs, the EM25 (EMissions around the M25) project focused on aircraft-based in situ observations of aerosols and trace gases and remotely sensed aerosol properties measured by a ground-based mobile lidar up- and downwind of Greater London. The mobile platforms travelled in circuits roughly encompassing the M25 motorway "ring road", shown in Fig. 1a. This approach allowed us to sample air upwind and downwind of London and compare the urban emissions with regional pollution moving over the city. Here we present an overview of major findings from the campaign to serve as a background for more detailed analyses of trace gas and aerosol properties.

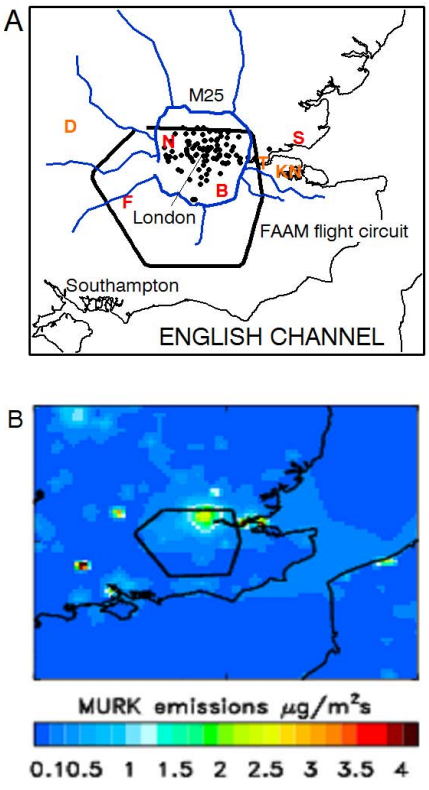

Fig. 1. Maps of south-eastern England showing: **(a)** location of the major motorway network (blue lines), London Air Quality Network observing sites (black circles), the main FAAM London circuit flight track (black line), the locations of three large coal-fired power stations (orange letters: "D" = Didcot; "T" = Tillbury; "KN" = Kings North) and airfields used for missed approaches (red letters: "N" = Northolt; "F" = Farnborough; "B" = Biggin Hill; "S" = Southend) and **(b)** "MURK" emissions (a generic term for emissions that drive the aerosol field in the UK4 model forecast).

Table 1. Summary of flights and synoptic conditions during the EM25 campaign.

Flight ID	Date	Time (UTC)	Regions sampled	Synoptic flow (850 hPa)
B457	16 June 2009	09:10–14:00	M25 circuits only	light westerly
B458	18 June 2009	09:50–14:45	M25 circuit and SE English coast	strong westerly
B459	22 June 2009	09:10–13:00	M25 circuits only	stagnant/light northerly
B460	23 June 2009	10:00–14:10	M25 circuits only	light easterly
B461	24 June 2009	08:45–12:00	M25 and English channel	strong easterly

London is located in south-eastern England in the United Kingdom (Fig. 1a) and has essentially a maritime climate. The major contributors to emissions in London depend on pollutant type. Road transport (52 % of total emissions including passenger cars, 17 %, and rigid heavy-duty vehicles, 13 %) and natural gas use (32 %) were the most important source types of nitrogen oxides (NO_x) within the M25 in 2004 according to the London Atmospheric Emissions Inventory (LAEI; Mattai and Hutchinson, 2008). Major VOC emission sources in the London region include the evaporation of industrial solvents and petrol (45 % total VOC emissions), road transport (30 %), and agricultural or natural sources including urban parks (20 %). The main contributors to the sources of particulate matter in London are road traffic (producing primary aerosol from both exhaust and non-exhaust emissions), primary particles from industry, and secondary particles from the oxidation of SO_2, NO_x and VOCs emitted by traffic and industry (Harrison et al., 2004). Transport of regional PM, such as aged organic aerosol, also contributes to London aerosol mass concentrations in addition to the local sources (Allan et al., 2010).

2 Methods

The EM25 campaign took place between 16–24 June 2009 in and around the Greater London region. In addition to a number of gas and aerosol long-term monitoring sites, the experiment featured two mobile measurement platforms, the UK Facility for Airborne Atmospheric Measurements (FAAM) modified BAe-146 research aircraft and a van fitted with a mobile lidar system, both described in detail below. The FAAM research aircraft flight tracks were designed to follow the M25 motorway as closely as possible at a minimum safe altitude of ∼750 m above ground level (a.g.l), but deviated in the western and southern portions of the circuit to comply with air traffic control restrictions owing to the proximity of the Heathrow and Gatwick terminal manoeuvring areas. Vertical profiles were obtained during each flight by flying "missed approaches" into Northolt, Farnborough, and Southport airfields (Fig. 1), selected based on the prevailing wind direction to probe the atmosphere to ∼20 m a.g.l. The research flights and lidar van deployments were coordinated to allow simultaneous sampling for the dates listed in Table 1.

2.1 FAAM research aircraft and instruments

The FAAM research aircraft is a BAe-146 jet modified for atmospheric measurements and has participated in a large number of campaigns since 2004. Real-time measurements of carbon monoxide, nitrogen oxides and ozone were made by an Aero-Laser AL5002 VUV resonance fluorescence gas analyser, a chemiluminescence gas analyser (Thermo Scientific Model 42) and a UV photometric gas analyser (Thermo Environmental Instruments Inc., USA, Model 49C), respectively. Calibration procedures for the real-time gas analysers are described by Hopkins et al. (2006). Whole air canister samples were collected in 3 L silica coated stainless steel canisters (Thames Restek, UK) using an all-stainless steel assembly double headed bellows pump (Senior Aerospace, USA), which drew air from the main sampling manifold of the aircraft and pressurised air into canisters to a maximum pressure of ∼3 bar. Samples were usually collected over approximately one minute intervals during selected portions of each flight. The samples were analysed off-line for VOCs using a dual channel gas chromatograph with flame ionisation detection (Hopkins et al., 2011).

Aerosol composition measurements were made by an Aerodyne compact Time-of-Flight Aerosol Mass Spectrometer (cToF-AMS) (Canagaratna et al., 2007; Drewnick et al., 2005; Morgan et al., 2010b) and a DMT Single Particle Soot Photometer (SP2) (Baumgardner et al., 2004; McMeeking et al., 2010; Schwarz et al., 2006). The AMS provided size-resolved chemical composition information for sub-micron, non-refractory particulate matter, classified as organic aerosol (OA), sulphate, nitrate, ammonium and non-sea salt chloride. The SP2 made size-resolved measurements of refractory black carbon (rBC) mass for "cores" between approximately 0.5–300 fg and also provided information regarding the rBC mixing state for a subset of the measured particles (Moteki and Kondo, 2007). The AMS was calibrated and data were analysed following the procedures described in detail by Morgan et al. (2010b). The SP2 data analysis followed the procedures described by McMeeking et al. (2010) and calibrations were performed using mobility diameter-selected glassy carbon spheres and polystyrene latex spheres (PSL).

Aerosol number distributions were measured by a wing-mounted passive cavity aerosol spectrometer probe

Table 2. Summary of in situ trace gas and aerosol sampling instrumentation on the FAAM BAe-146 during the EM25 campaign.

Quantity measured	Instrument	Size range or wavelength	Uncertainty
CO	Aero-laser 5002	N/A	±1.5 ppbv at 100 ppbv
NO, NO_2	Thermo model 42C	N/A	±5 ppbv
O_3	Thermo model 49C	N/A	±3 ppbv
C_2-C_8 volatile organic compounds	whole air sampler (WAS) + off-line gas chromatography	N/A	variable, see Hopkins et al. (2011)
aerosol composition and mass	Aerodyne time-of-flight aerosol mass spectrometer (AMS)	∼50–800 nm	∼25 %, see Canagaratna et al. (2007)
refractory black carbon aerosol mass	DMT single particle soot photometer (SP2)	∼70–600 nm	∼30 % for rBC, see Schwarz et al. (2008)
aerosol optical diameter and concentration	passive cavity aerosol spectrometer probe (PCASP-100X, SPP200); cloud aerosol spectrometer (CAS)	0.1–3 µm; 0.5–50 µm	±20 % (diameter) ±15 % (concentration)
aerosol concentration	TSI 3786 water-based ultrafine condensation particle counter (WCPC)	> 3 nm	±12 %
dry aerosol light scattering coefficient	TSI 3563 integrating nephelometer	λ = 450, 550, 700 nm	±10 %, see Anderson et al. (1996)
"wet" aerosol light scattering coefficient	"wet" TSI 3563 integrating nephelometer	λ = 450, 550, 700 nm	> 10 %
aerosol light absorption coefficient	particle soot absorption photometer (PSAP)	λ = 567 nm (corrected to 550 nm)	variable, see Bond et al. (1999); Lack et al. (2008)

(PCASP-100X with SPP-200 hardware upgrade), which optically counted and sized particles between 0.1 and 3μ diameter. Particle size bins up to 0.8 µm were calibrated using ammonium sulphate, which was converted to a PSL-equivalent diameter using Mie theory. Coarse mode aerosol and cloud hydrometeors in the size range 0.5–50 µm diameter were counted and sized using a DMT cloud aerosol spectrometer (CAS) operating as part of a wing-mounted DMT cloud, aerosol and precipitation spectrometer (CAPS) probe. Daily checks of the CAS size calibration were performed using glass beads. Aerosol number concentrations (diameter >3 nm) were measured by a modified TSI 3786 ultrafine water-based condensation particle counter (WCPC).

Wet and dry aerosol light scattering (b_{sp}) and ambient absorption (b_{ap}) coefficients were measured by two TSI 3563 integrating nephelometers (Haywood et al., 2008a) and a particle soot absorption photometer (PSAP). The PSAP and nephelometer sample air through the same inlet and heating associated with bringing the sample into the aircraft reduces the sample RH. Measurements of RH at the nephelometer inlet indicate the sample RH was typically below 30 % (Highwood et al., 2011). The dry and wet nephelometer measurements were corrected for angular truncation and non-Lambertian light-source errors using the submicron correction parameters provided by Anderson and Ogren (1998). The nephelometer system performed scans between 40–90 % relative humidity (RH) to determine the light scattering growth factor or f(RH) (Morgan et al., 2010a). The average scan cycle (up and down) took between 10–30 min to complete. We corrected the scattering coefficients to ambient conditions based on the measured relative humidity and the average f(RH) response observed over the entire study. The PSAP measurements were corrected following Bond et al. (1999) to account for variations in the particle deposit spot size, instrument flow rate and adjust the measurement to 550 nm wavelength for comparing with the 550 nm nephelometer wavelength.

All on-board aerosol instruments sampled ambient air via stainless steel tubing through Rosemount inlets. The inlet efficiency for super-micron particles is believed to be low (Haywood et al., 2003), so the aircraft measurements are thought to represent predominantly sub-micron aerosol properties. Aerosol number and mass concentrations, scattering and absorption coefficients are reported at standard temperature and pressure (STP) defined as 273.15 K and 1013.25 hPa. For clarity, these parameters are denoted using an "s" (e.g., $s\,m^3$) to distinguish them from ambient concentrations and coefficients. All real-time measurements were averaged to the approximately 30 s time resolution of the AMS or the sampling interval of the whole air canister

samplers, if collected. Table 2 summarizes the instruments and associated uncertainties used during the project.

2.2 Ground-based mobile LIDAR

We used a mobile Aerosol LIDAR System (ALS) to investigate the aerosol vertical distribution around London. The ALS is a custom-built backscatter lidar emitting in the ultraviolet developed by the Commissariat à l'Energie Atomique (CEA) and the Centre National de la Recherche Scientifique (CNRS) (Chazette et al., 2007). It is available commercially from the LEOSPHERE Company under the name of EZ Lidar® (www.leosphere.com). It is designed to monitor the aerosol dispersion in the low and middle troposphere and operated with a Nd:YAG laser at the wavelength of 355 nm. The detection system had parallel and cross-polarised detection channels. The resolution along the line of sight was 15 m for a sampling of 1.5 m and had an overlap factor close to 1 at approximately 150 m above the ground level.

The primary ALS measurement is the backscatter coefficient measured at 355 nm, which has both molecular (i.e., gas-phase) and aerosol contributions. It is mounted in a small vehicle allowing it to follow small atmospheric features (Raut and Chazette, 2009; Royer et al., 2011b), provide information regarding the vertical distribution of aerosols around London by following a set loop following the M25 ring-road or beltway, and could examine the role of the M25 traffic in the production of anthropogenic aerosols. The lidar signals have been calibrated, corrected from the background sky radiance and range-corrected. We retrieved aerosol extinction coefficients from the measured backscatter coefficients following the procedures described by Raut and Chazette (2007) and Royer et al. (2011a), assuming a lidar ratio of 45.5 sr. Extinction coefficients were estimated at 550 nm by assuming an Ångström exponent of 1.5. Uncertainties associated with the retrieval of aerosol extinction coefficient at 355 nm were due to four main sources: (a) statistical fluctuations of the measured signal, associated with the random detection process, (b) uncertainty in the lidar signal in the altitude range used for the normalization, (c) the uncertainty of the a priori knowledge of the vertical profile of the molecular backscatter coefficient as determined from ancillary measurements and (d) the uncertainty in the backscatter to extinction ratio (or lidar ratio) and its altitude dependence. Chazette et al. (2010) discuss the different sources of uncertainty and conclude that there is an absolute error of approximately $0.01\,km^{-1}$ in the retrieved aerosol extinction coefficient. We assumed a lidar ratio of ∼45 sr based on similar retrievals of extinction coefficients in a polluted boundary layer in Paris (Chazette et al., 2012).

2.3 Ground-based fixed measurements

In addition to the aircraft and ground-based lidar measurements, we used three networks of ground-based measurements across London to provide information on aerosol distribution within the circuits performed by the mobile measurements. The first was a well-established network of air quality measurements run by the London Air Quality Network (http://www.londonair.org.uk) (Atkinson et al., 2009; Fuller and Green, 2006), which includes measurements of PM_{10} concentrations at most stations, and $PM_{2.5}$ at a subset of these measured with a Tapered Element Oscillating Microbalance (see Fig. 1a). The stations represent a variety of site types, including suburban, urban background, industrial, roadside and kerbside locations. Second, we analysed data from a new network of weather stations which was set up as part of the OPen Air Laboratories (OPAL) project (Davies et al., 2011). The weather stations are Davis Vantage Pro2 Plus automatic weather stations measuring standard meteorological variables, although during EM25 measurements of solar irradiance were used to infer column aerosol loadings on clear days (Ryder and Toumi, 2011). The third network included two locations that are part of the UK Automated Hydrocarbon Network, a kerb-side site (Marylebone Road) and a suburban site (Eltham). Both sites feature automatic Perkin Elmer gas chromatograph systems measuring over 25 different hydrocarbon species (http://www.uk-air.defra.gov.uk).

3 Results and discussion

3.1 Meteorology and transport

Flight operations during the June 2009 EM25 campaign window targeted polluted conditions to assess pollution transport into and out of the London region. Meteorological conditions during the five flight days are summarized in Fig. 2, which shows the 850 hPa geopotential height fields and 850 hPa pressure level winds from the ECMWF ERA Interim reanalysis. The first two flights on 16 and 18 June took place before and after the passage of a precipitating cold front over the UK. The 850 hPa pressure-level winds on 16 June over the London region were light and variable, though generally westerly or southwesterly, changing to westerly on 18 June following the passage of a front the previous night. The final three flights took place between 22–24 June, when a high pressure system moved eastwards from southern Ireland to southern Norway. Flow over the London region changed from light northerlies on 22 June to easterlies on 23–24 June. There were usually scattered fair weather cumuli clouds over the study region with no precipitation on flight days, though cloud base was above the flight measurement altitude for all but a few brief periods, which have been removed from the analysis.

We examined aerosol mass concentrations measured by the ground stations to provide context for the aircraft measurements during the EM25 campaign. Figure 3 shows $PM_{2.5}$ concentrations from the London ground stations shown in Fig. 1a with summertime (June/July) mean values for the

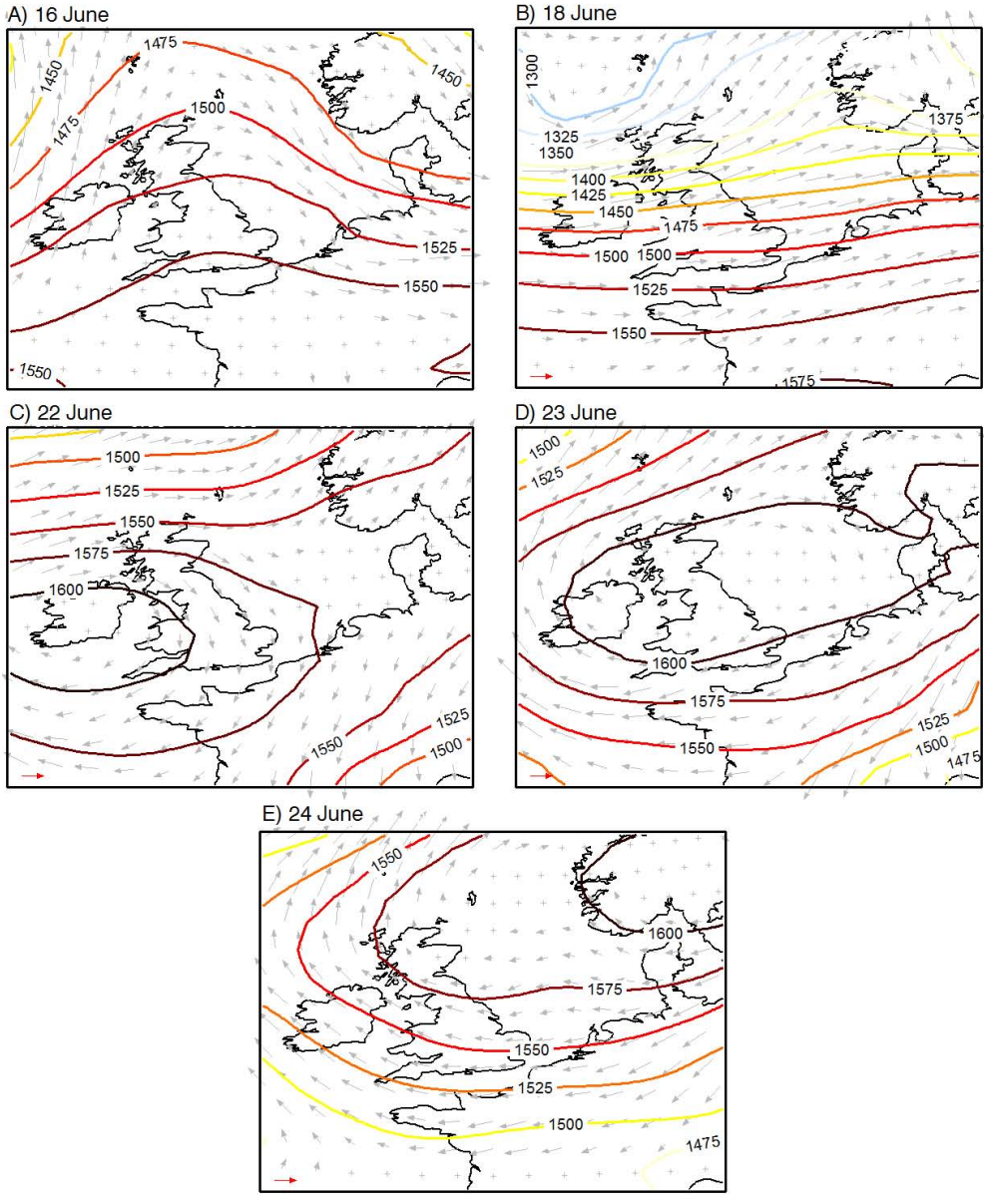

Fig. 2. Maps showing geopotential height and winds from the ERA Interim ECMWF re-analysis at the 850 hPa pressure level at 12:00 UTC for each flight day. Red arrow in lower left-hand corner indicates 10 m s^{-1} wind speed.

period 2005–2009. Mass concentrations were near or slightly below their July/July 2005–2009 averages (approximately 15 µg m^{-3}) from 16 June to 22 June. $PM_{2.5}$ concentrations then increased to above average (20 µg m^{-3}), reflecting the change from predominantly westerly to easterly winds and associated transport of pollution from continental Europe (Bigi and Harrison, 2010).

Forecast aerosol mass concentrations from the 4 km resolution operational numerical weather prediction (NWP) model (Clark et al., 2008; Haywood et al., 2008b) showed transport patterns and expected pollution "hotspots" in the London area. In addition to providing standard meteorological variables such as temperature, humidity, cloud and precipitation fields, the UK4 model included a highly simplified representation of aerosol emission, transformation, and deposition (Clark et al., 2008). Sources of aerosol were based on the European emission inventory on a 1/8 degree by 1/16 degree grid developed for the GEMS project by Visschedijk et al. (2007) plus ship emissions from the European Monitoring and Evaluation Programme (EMEP) emissions database for 2005. The aerosol was represented by a single tracer (generically termed "murk") which approximately accounted for sources from SO_2, NO_x and VOCs by using a factor representing the average conversion of the gas emissions to

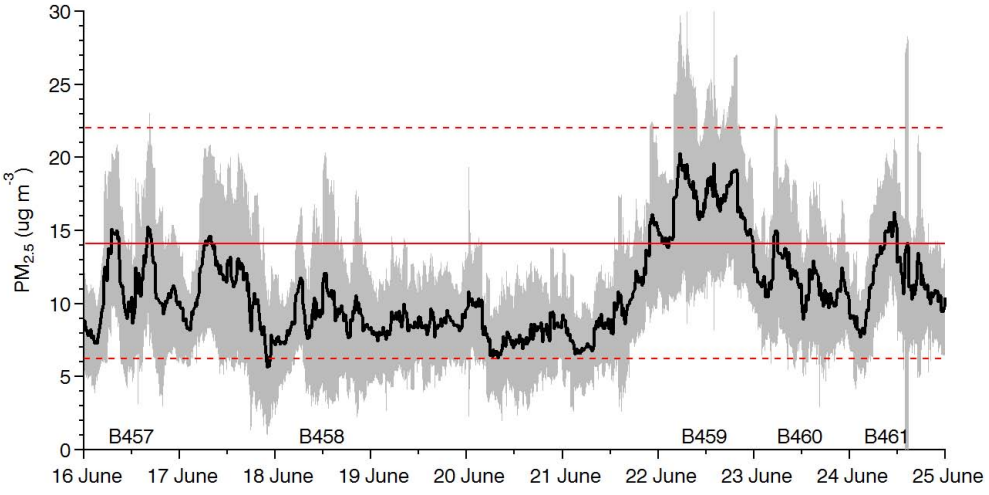

Fig. 3. Time series showing $PM_{2.5}$ concentrations during the EM25 campaign period in 2009. Heavy black line shows London average for all PM stations over the EM25 campaign and grey shading shows one standard deviation of the average. Solid red line shows the June/July historical London average $PM_{2.5}$ concentration from 2005 to 2009 (all station classifications) and dashed red lines show two standard deviations. Flight identification numbers indicate days when the FAAM BAe-146 research aircraft flew circuits over London. Date ticks are labelled at 00:00 UTC for that day.

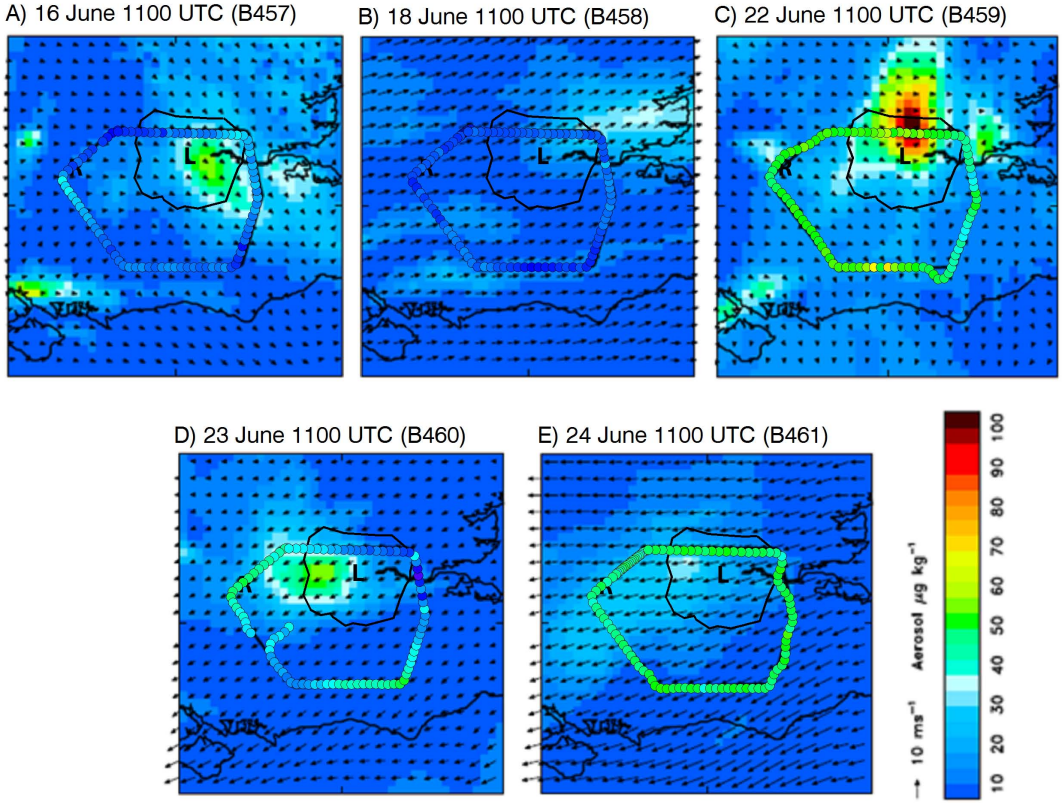

Fig. 4. Aerosol mass mixing ratios predicted at the 760 m altitude by the UK 4km visibility model for selected times during each flight day. Arrows indicate wind speed and direction at the predicted level. The "R" indicates the location of the city of Reading and "L" indicates the location of central London. Flight tracks for each day are shown by filled circles, shaded by total aerosol mass measured on the aircraft. Aircraft mass concentrations are shaded similar to model fields but multiplied by a factor of four.

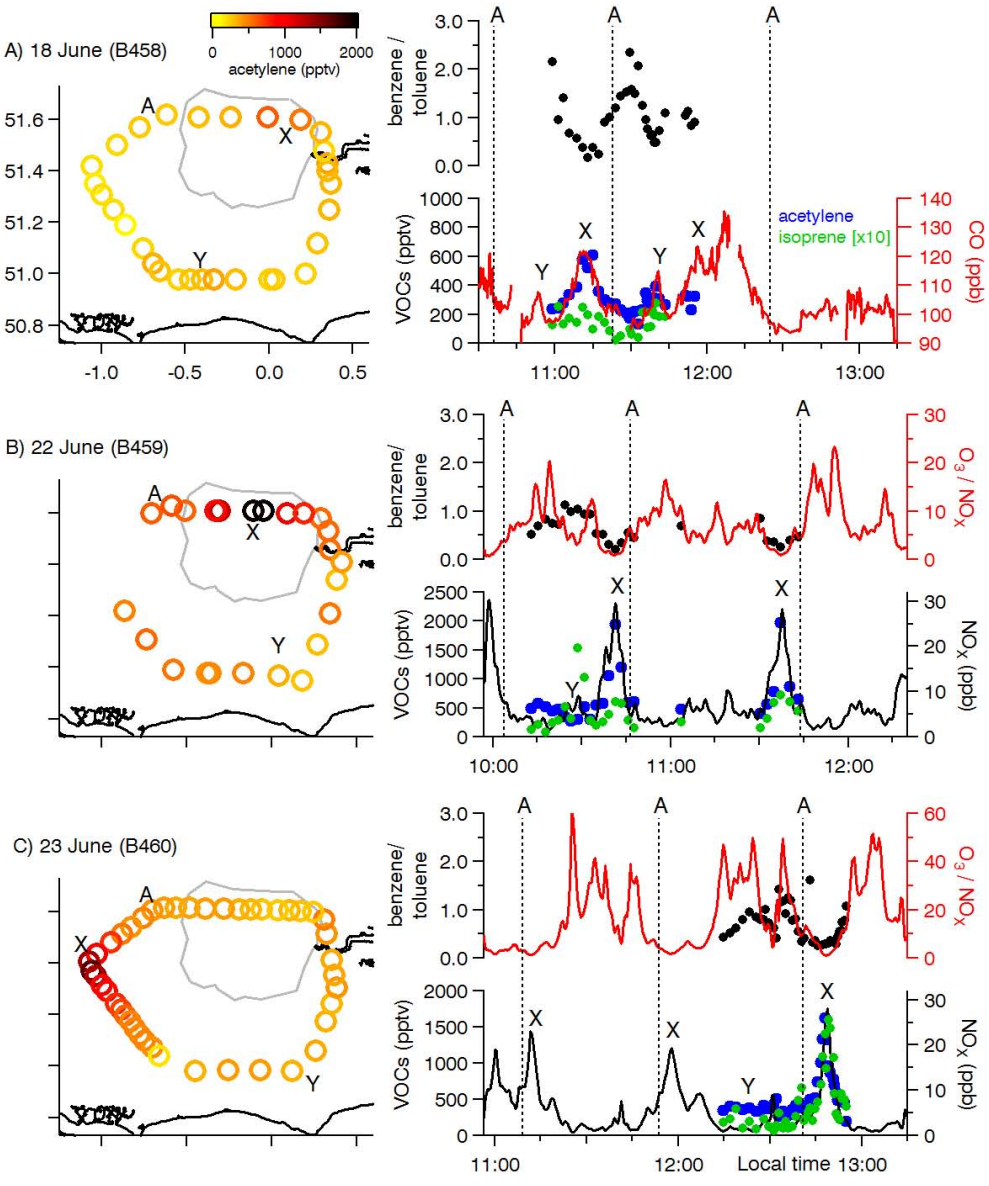

Fig. 5. Mixing ratios for acetylene (C_2H_2), isoprene, nitrogen oxides (NO_x), carbon monoxide and ratios of ozone-to-nitrogen and benzene-to-toluene measured around London for three EM25 flights. NO_x mixing ratios were unavailable for the 18 June flight so CO is shown instead. The approximate location of the London plume is indicated by "X". Additional features of interest are shown by "Y". Point "A" on each map corresponds to the dashed lines on each time series. The flight direction for all days was anti-clockwise.

aerosol within the model domain. The emission fields used by the model are shown in Fig. 1b. The aerosol concentration was used along with a mean hygroscopic growth factor to provide forecasts of atmospheric visibility (Haywood et al., 2008b). The hygroscopic growth factor used was based on nephelometer data from previous flight campaigns. Variational data-assimilation of observed visibilities were used to correct the model fields of aerosol mass concentration and relative humidity (Clark et al., 2008).

Snapshots of the predicted aerosol mass distribution together with segments of flight tracks shaded according to aircraft-measured sub-micron aerosol mass concentrations are shown in Fig. 4 for illustrative purposes timed at approximately the middle of aircraft circuits. At the 760 m model level nearest to the aircraft altitude during circuits, the highest aerosol emissions were predicted to be around London. The predicted plume advected southeast and east for the northwesterly and westerly flights (16 and 18 June; Fig. 4a and b), west for the two easterly flow cases (23 and 24 June; Fig. 4d and e) and remained over the London region and slightly to the north for the stagnant 22 June flight (Fig. 4c). Plumes from the Southampton area to the

southwest of London may have reached the flight track for the 16 and 18 June flights. The visibility model also showed emissions from the coal-fired Didcot power station (shown in Fig. 1a) possibly reaching the flight track on 16, 22 and 23 June. The model predicted the highest and lowest aerosol concentrations over London on 22 and 18 June, respectively.

We classified different portions of each flight as either "plume", "regional" or "upwind" based on measurements of rBC mass concentrations from the SP2 and predicted wind fields. Plumes were defined as regions having rBC mass concentrations greater than the 75th percentile for the flight downwind of London. Upwind regions were determined from model predicted wind fields while regional samples included all periods when rBC mass concentrations were below the 75th percentile, including upwind regions.

3.2 Trace gas measurements

Three flights (B458, B459 and B460) had valid trace gas measurements from the whole air sampling system, shown in Fig. 5. Major features, such as increases in VOCs, were consistent during repeat flight circuits. All circuits had peaks in CO (and NO_x if measured) mixing ratio(s) and decreases in the ozone mixing ratio when the aircraft was in the London plume, denoted by the letter "X" in Fig. 5a–c. Mixing ratios of CO have a background contribution that we estimated from the intercept of the regression of CO on rBC measured by the SP2. Background CO values were between 90–98 ppb and we subtracted these background values to obtain excess mixing ratios for CO for each flight (ΔCO). Acetylene (C_2H_2) was elevated in the London plume and was highly correlated with CO ($r^2 = 0.86$) and NO_x ($r^2 = 0.79$). Acetylene is primarily emitted as vehicle exhaust (Fortin et al., 2005) and has a relatively long atmospheric lifetime of approximately 2 months with respect to oxidation by OH (Atkinson, 2000). Figure 5 also shows the ratio of benzene-to-toluene, which is commonly used to determine the air mass photochemical age because of the different atmospheric lifetimes of the two species (e.g., Warneke et al. 2007). The regions with low benzene/toluene ratios and elevated pollutant concentrations coincided with the location of the aerosol plume predicted by the UK visibility model and expected based on flow patterns from the synoptic re-analysis, i.e., downwind of London. We also observed elevated CO and VOC concentrations away from the London plume together with increased ozone relative to NO_x. These locations had slightly higher benzene/toluene ratios, suggesting they were more aged regional pollution or aged plumes from non-London sources encountered by the aircraft. We identify these features for selected flights in Fig. 5a–c using the letter "Y".

We estimated initial emission ratios for various VOCs relative to acetylene and CO using a simple linear regression approach. Other methods compare VOC ratios to photochemical age (t_{photo}) to account for changes in VOC concentrations with time due to photochemical reactions (e.g., Warneke et al., 2007). We also calculated emission ratios using the photochemical age method, but only report the linear regression results because of uncertainties in the initial benzene-toluene ratio at the source region and the OH radical concentrations. We did use an estimate of photochemical age to examine aerosol properties as a rough function of time and to provide a second set of emission ratios restricted to samples with photochemical age of less than 20 h to better represent the London emissions. We estimated the photochemical age by assuming a concentration of hydroxyl radical (2×10^6 molecules cm^{-3}) and an assumed initial toluene/benzene ratio of 5 for London needed for the calculation. The absolute accuracy of the photochemical age was not critical to the analysis because we sought to roughly distinguish fresh and aged air masses. We performed the calculations for data combined from all three flights where VOC data from whole air samplers were available (18, 22, and 23 June).

Emission ratios of various VOCs to acetylene determined from linear regression are listed in Table 3 together with an associated measure of correlation (Pearsons r^2) for all samples and for those with photochemical age less than 20 h. We compared emission ratios calculated for the "fresh" London emissions (t_{photo} <20 h) to several previously published

Table 3. Emission ratios for selected volatile organic compounds with respect to acetylene measured and associated coefficient of variation for all EM25 samples and for the subset with photochemical age less than 20 hours. Atmospheric lifetimes with respect to oxidation by OH at a concentration of 2×10^6 molecules cm^{-3} reported by Atkinson (2000) are listed for selected species.

compound	τ	X/C_2H_2	r^2	X/C_2H_2	r^2
		all		t_{photo} <20 h	
acetylene	2 mo	1.0	1.0	1.0	1.0
ethane	3 mo	3.09	0.86	3.41	0.85
n-butane	4.7 d	1.27	0.75	1.21	0.97
propane	10 d	1.24	0.43	1.31	0.96
iso-butane	7.5 d	0.74	0.86	0.71	0.97
iso-pentane	5 d	0.73	0.57	0.57	0.54
toluene	1.9 d	0.55	0.90	0.47	0.86
ethene	1.4 d	0.52	0.77	0.45	0.82
m+p-xylene	5.9 h	0.27	0.84	0.27	0.91
n-pentane	5 d	0.23	0.32	0.19	0.43
2, 3-methylpentane		0.19	0.67	0.18	0.93
benzene	9.4 d	0.11	0.91	0.11	0.93
propene	5.3 h	0.10	0.60	0.10	0.91
ethylbenzene		0.07	0.51	0.08	0.78
n-hexane		0.07	0.61	0.07	0.85
isoprene	1.4 h	0.06	0.35	0.04	0.18
cyclopentane		0.05	0.55	0.04	0.86
o-xylene		0.03	0.01	0.04	0.01
1-butene		0.02	0.50	0.01	0.28
trans-2-butene	2.2 h	0.01	0.38	0.01	0.67
cis-2-butene		0.00	0.46	0.00	0.40

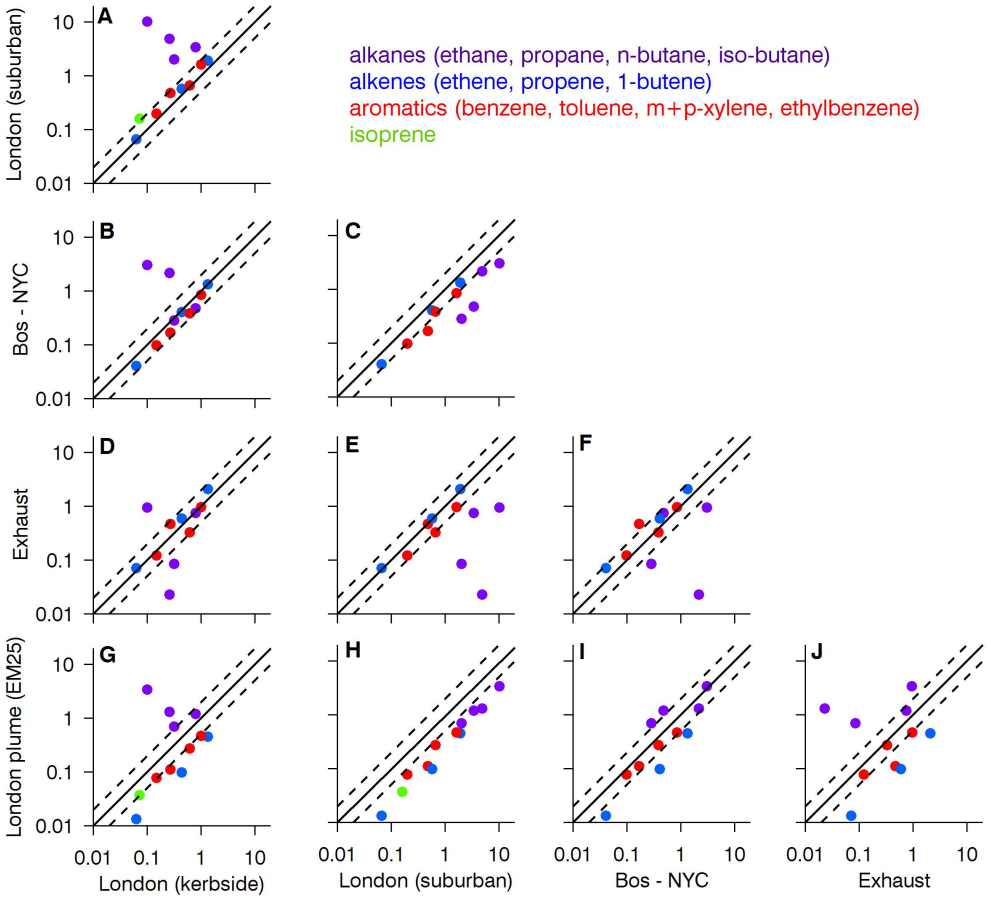

Fig. 6. Selected volatile organic compound (VOC) emission ratios to acetylene (C_2H_2) measured on the FAAM BAe-146 research aircraft for samples with photochemical age less than 20 h, at ground sampling sites in London, and by previous measurement campaigns. Bos-NYC refers to emission ratios measured in the outflow of the north-eastern US reported by Warneke et al. (2007), exhaust refers to vehicle exhaust emission ratios reported by Harley et al. (1992), and the London (kerbside) and London (suburban) data were obtained from the Marylebone Road and Eltham automated hydrocarbon monitoring network locations for June/July 2008–2010. Points are shaded by VOC family as alkanes, alkenes and aromatics. The solid line gives the 1:1 relationship and the dashed lines 2:1 and 1:2 relationships; all axes are log-scaled and identical.

emission ratios for cities in the north-eastern US (Warneke et al., 2007), emissions directly measured from petrol vehicle exhaust (Harley et al., 1992) and ratios we calculated from measurements at two automatic hydrocarbon monitoring sites in London. The London monitoring locations were Marylebone Road in central London, which is classified as a kerb-side site, and Eltham in eastern London, which is classified as a suburban site. We calculated emission ratios by regressing selected VOCs against acetylene for measurements in June and July between 2008 and 2010 to compare to our June 2009 aircraft observations because both London sites had measurement gaps during the EM25 campaign.

We compare VOC to acetylene emission ratios from different studies and sites to each other in Fig. 6. Each row and column in the figure contains a scatter plot that compares VOC to acetylene ratios measured at a particular site or for a particular study to another site or study. For example Fig. 6f compares VOC ratios measured for vehicle exhaust by Harley et al. (1992) to those measured downwind of the north-eastern US by Warneke et al. (2007). VOC emission ratios to acetylene measured by the aircraft were correlated with those determined for the London monitoring sites (Figures 6g and 6h), but the ratios measured at the ground sites were approximately twice those measured aloft. We suspect these differences arise from the larger influence of entrainment on the aircraft measurements and the different lifetimes of the VOCs. Short-chain alkanes (particularly ethane and propane) measured at the Marylebone Road site were the exception to this trend, having much lower ratios compared to those measured by the aircraft and at the suburban site (Fig. 6a and g). The short alkanes have a large evaporative fuel contribution and previous studies have suggested that this explains the lower ratios observed downwind of urban regions compared to vehicle emissions (de Gouw et al., 2005).

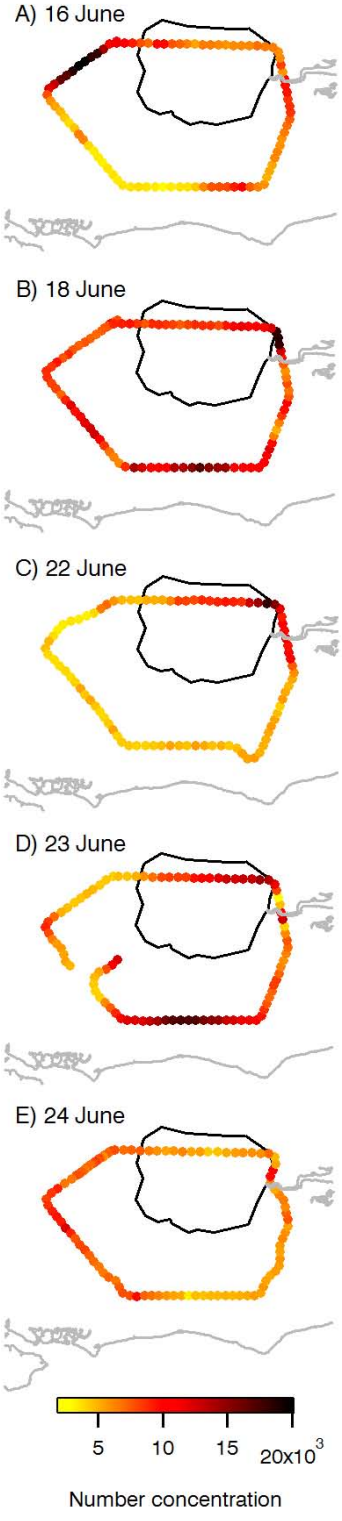

Fig. 7. Number concentrations for particles with $D_p > 3$ nm measured by the ultrafine water-based condensation particle counter for single circuits around London during each flight. Note scale on panel **(d)** has been adjusted by a factor of 2 (maximum $N = 40\,000\,cm^{-3}$) to better illustrate the variability along the flight path.

The aircraft alkane to acetylene emission ratios were lower than those measured at the suburban Eltham site (Fig. 6h), which is less vehicle emission dominated than the Marylebone Road location. The alkane to acetylene emission ratios were also statistically less certain because of the low coefficients of variation observed in both the aircraft and ground monitoring site data.

Warneke et al. (2007) concluded that emissions of aromatics and alkenes are dominated by vehicle exhaust, at least for urban areas in the north-eastern US, based on the relatively good agreement between emission ratios to acetylene measured for urban outflow and those reported for petrol engine vehicle exhaust by Harley et al. (1992) (Fig. 6f). We found similar agreement between aircraft-measured and vehicle exhaust emission ratios for aromatics, but poorer agreement for alkene emissions (Fig. 6j), which may arise from the influence of the entrainment of air with lower alkene-to-acetylene ratios on the aircraft measurements. Alkene to acetylene emission ratios measured at both London ground sites were in excellent agreement with vehicle exhaust (Fig. 6d and e), suggesting that increasing differences in fleet composition in the US and Europe are not affecting emission ratios. For example, diesel consumption in the Greater London region in 2009 was approximately equal to that of petrol (UK Department of Energy and Climate), but it was approximately 15 % of petrol consumption in California in the first quarter of 2011 (California State Board of Equalization).

Despite differences in timing, sampling method and analytical approach, we observed VOC to acetylene emission ratios in London outflow that are within a factor of two of those reported for the north-eastern US by Warneke et al. (2007) (Fig. 6i). They reported observations within a factor of two of those reported for 39 US cities by Seila et al. (1989). These findings provide further support to recent analyses that indicate VOC to acetylene emission ratios from cities, at least in the locations that have been characterised, are generally consistent, despite differences in location, vehicle fleets, and photochemical environments. For example, Parrish et al. (2009) compared relationships between different VOC mixing ratios for observational datasets collected in several mega-cities and in many US cities. They found nearly identical (0.29–0.31) benzene-acetylene ratios in Mexico City, Tokyo, Beijing and 71 US cities (measured in the 1980s), but lower ratios for recent measurements in the north-eastern US (0.17). von Schneidemesser et al. (2010) found yearly-averaged benzene-acetylene ratios for 2000–2008 between 0.17–0.29 for London. Benzene-acetylene ratios we measured in London outflow were even lower than reported for the north-eastern US (0.11) however the ratios determined for the ground site locations were higher, between 0.3–0.5. Parish et al. (2009) attributed the lower ratios observed in the north-eastern US to targeted benzene reductions following the 1990 Amendments to the Clean Air Act. Similar benzene emission reductions were implemented in the UK in the 1990s and benzene levels in the UK were dropping by

approximately 20 % per year until at least 2005 (Dollard et al., 2007). Our own analysis of Marylebone Road data indicated that the ratio of benzene to acetylene since 2000 was approximately constant at ∼0.2 until 2008 but has increased to approximately 0.4 since then, which may be related to changes in the vehicle fleet in London. According to Parrish et al. (2009), the similar ratios for various megacity VOC emission ratios across the world result from a combination of the fact that vehicular emissions and associated fuel evaporation dominate emissions and that the hydrocarbon composition of petrol and exhaust emissions is consistent over these urban areas. Though there are some discrepancies in emission ratios measured by the aircraft and those from the ground-based monitoring stations, we found no evidence of a major difference between the London emission ratios and those reported for other highly-developed urban regions.

Isoprene is a major biogenic VOC that also has both vehicular and other anthropogenic sources. Langford et al. (2010) performed eddy covariance VOC flux measurements over London and also analysed long-term Marylebone Road VOC observations to conclude that as much as 80 % of isoprene in London has biogenic sources on warm (30 °C) days. We compared isoprene to benzene (not shown) to identify periods of the flight when isoprene became elevated with respect to benzene. Two portions of different flights showed large increases in isoprene mixing ratios in the absence of changes in benzene and other anthropogenic pollution tracers, both occurring over the southern portion of each flight circuit (Fig. 5). We believe both of these events were associated with increased emissions from the more rural landscape south of the M25 region rather than emissions from London itself based on the wind flow patterns during each flight. We also observed increases in isoprene mixing ratios over London that were coincident with increases in benzene. Average maximum temperatures in London on the days of our measurements were between 18–25 °C, which corresponds to a 20–60 % expected temperature-dependent/biogenic isoprene contribution (Langford et al., 2010). We observed slightly higher isoprene relative to benzene on 23 June (maximum temperature ∼25 °C) compared to 22 June (maximum temperature ∼22 °C) consistent with this view. A recent analysis by von Schneidemesser et al. (2011) has shown that despite recent reductions in anthropogenic non-methane hydrocarbons (NMHCs) the contribution of isoprene to NMHC OH reactivity has not gained importance in urban London. They attribute this result in part to the fraction of isoprene emitted by anthropogenic sources.

3.3 Aerosol physical properties

Aerosol number distributions measured by the PCASP and CAS wing-mounted probes had a dominant accumulation mode (centred at approximately 0.17 µm)with only minor contributions from coarse particles (optical diameter >1 µm) to total number and volume in the London circuits. The campaign-average standard deviation of the number distributions was best represented by a log-normal distribution with mean diameter 0.17 µm and a standard deviation of 1.4. We observed little change in aerosol number size distributions around the circuit, consistent with relatively homogeneous sub-micron aerosol mass concentrations and light scattering coefficients that were measured by the AMS and nephelometer, respectively. Kleinman et al. (2009) conducted size distribution measurements over Mexico City and observed minor changes in the size distribution but did observe changes in the number of particles in the accumulation mode that were correlated with changes in particle mass and carbon monoxide. Changes in total number concentrations measured by the ultrafine CPC (diameter >∼3 nm) partly reflected changes in sub-0.1 µm particles because they dominate number distributions, giving us some indication of their distribution around London during the flights. The regions of high particle number concentrations shown in Fig. 7 were not always co-located with the urban plume identified from the rBC mass concentrations. We observed a correlation between particle concentrations and sulphur dioxide (SO_2) mixing ratios, particularly downwind of coal-fired power plants in the vicinity of London, including the Didcot, Tilbury and Kings North power stations shown in Fig. 1b. These observations were consistent with the well-documented formation of fine sulphur containing particles downwind of SO_2 sources (e.g., Hewitt, 2001) and indicate that at least under typical summertime conditions power plant can have a similar contribution to particle number as the urban emissions in the London area.

Aerosol dry scattering coefficients were correlated with total sub-micron mass (sum of AMS mass and SP2 rBC) for all five flights (Pearson's $r^2 = 0.70$). The ratio of dry scattering coefficients measured at $\lambda = 550$ nm to sub-micron mass yielded a study-average mass scattering efficiency of $3.4\,m^2\,g^{-1}$, consistent with values expected for sub-micron dominated mixtures of OA, ammonium sulphate and ammonium nitrate and similar to the dry mass scattering efficiency of $3.6 \pm 1.3\,m^2\,g^{-1}$ reported for $PM_{2.5}$ over the eastern United States (Shinozuka et al., 2007). We also calculated the scattering and absorption coefficients from size distributions using Mie theory. The bulk, campaign-average aerosol refractive index and density, estimated from particle composition data by a volume-weighted mixing approach, were $1.59–0.022i$ and $1.63\,g\,cm^{-3}$, respectively. The average mass scattering efficiency determined from the Mie calculations was $3.5\,m^2\,g^{-1}$, in agreement with the measured value. The scattering efficiency around London was lower than the range of $4.5–5.9\,m^2\,g^{-1}$ for urban aerosols retrieved over the Paris region by Raut and Chazette (2009).

The humidity-dependence of light scattering coefficients (f(RH)) over London was generally weaker than that measured by the same equipment for a sulphate dominated aerosol over the eastern Pacific, shown in Fig. 8. The f(RH) was similar to that retrieved by Randriamiarisoa et al. (2006)

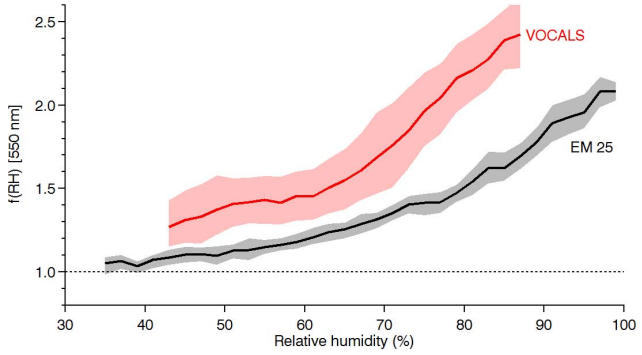

Fig. 8. Campaign-averaged ratios of humidified-to-dry corrected light scattering coefficients for 550 nm as a function of relative humidity during the EM25 (London, black) and VOCALS (south-eastern Pacific, red, Allen et al., 2011) campaigns. Solid lines indicate the median values and the shaded region shows the inter-quartile range. Dashed line shows no change in light scattering upon humidification.

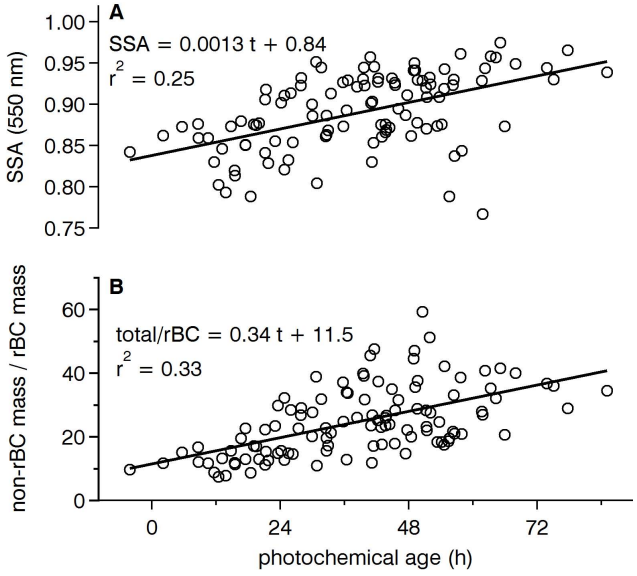

Fig. 9. Campaign-averaged ratios of humidified-to-dry corrected light scattering coefficients for 550 nm as a function of relative humidity during the EM25 (London, black) and VOCALS (south-eastern Pacific, red) campaigns.

for air masses passing over Paris that originated from the UK. Shinozuka et al. (2007) measured $f(\mathrm{RH})$ over North America and parameterized the scattering response measured at $\mathrm{RH}_1 = 40\,\%$ and $\mathrm{RH}_2 = 80\,\%$ using:

$$f(\mathrm{RH}) = \left(\frac{1-\frac{\mathrm{RH}_1}{100}}{1-\frac{\mathrm{RH}_2}{100}}\right)^{-\gamma} \quad (1)$$

where γ captures the effects of chemistry, mixing state, size and refractive index. We found that$\gamma \sim 0.3$ best fit the average $f(\mathrm{RH})$ observed over London, which is near the lower range of the Shinozuka et al. (2007) column-averaged values. The lower humidity-dependence of scattering was also consistent with higher mass fractions of relatively hydrophobic OA measured over London compared to the eastern Pacific (Allen et al., 2011), which have been shown in laboratory studies to suppress hygroscopic growth when internally mixed (e.g., Svenningsson et al., 2006). The growth factor differed from ∼2/3 of the ammonium sulphate-dominated aerosol sampled over the Pacific, showing the importance of treating the aerosol as an internal rather than external mixture.

Aerosol absorption coefficients were correlated with rBC mass concentrations measured by the SP2 for all five flights (Pearson's $r^2 = 0.67$). The regression for all non-profile measurements yielded an rBC mass absorption efficiency (MAE) at 550 nm of $10.4\,\mathrm{m^2\,g^{-1}}$, higher than the $7.5\pm1.2\,\mathrm{m^2\,g^{-1}}$ value recommended by Bond and Bergstrom (2006) for uncoated BC particles. Subramanian et al. (2010) reported an MAE of $13.1\,\mathrm{m^2\,g^{-1}}$ for rBC measured by an SP2 and a 3-wavelength PSAP over and downwind of Mexico City. Their MAE included an SP2 mass scaling factor of 1.3 to account for rBC mass falling outside the detection range of the instrument. When we applied the same correction to our data, we obtained an MAE of $7.8\,\mathrm{m^2\,g^{-1}}$ for London, almost a factor of two lower than that observed over and downwind of Mexico City. Baumgardner et al. (2007) reported a lower MAE of $5\,\mathrm{m^2\,g^{-1}}$ from an SP2 and PSAP in Mexico City than we observed, but their observations were made on the surface and very close to rBC sources. Both field (Lack et al., 2008) and laboratory (Cappa et al., 2008) observations have shown that the PSAP measures erroneously high absorption coefficients for high OA loadings, so the lower MAE observed by the PSAP/SP2 combination over London may be partially due to the lower contribution by OA to sub-micron aerosol mass (∼30 %) around London compared to roughly 60 % contribution observed over Mexico City (DeCarlo et al., 2008).

We calculated the aerosol single scattering albedo (SSA), the ratio of the light scattering coefficient to the light extinction (scattering plus absorption) coefficient, from the corrected PSAP and nephelometer observations at $\lambda = 550$ nm around each circuit. The SSA decreased to 0.85 ± 0.03 (mean ±1 standard deviation) in the London plumes from a higher regional background of 0.91 ± 0.05 (Table 4), which was consistent with the higher light-absorbing rBC mass fractions in the plume compared to background regions of the circuit. Raut and Chazette (2007) obtained similar behaviour within and outside of the Paris plume. We investigated the timescales for increases in SSA by comparing its measured values to photochemical age for periods with valid whole air canister samples, shown in Fig. 9. Single scattering albedo increased from approximately 0.84 at $t = 0$ to approximately 0.95 at $t \sim 3$ days, consistent with the plume versus non-plume differences and the addition of secondary material including SOA indicated by the increase in the OA/ΔCO and

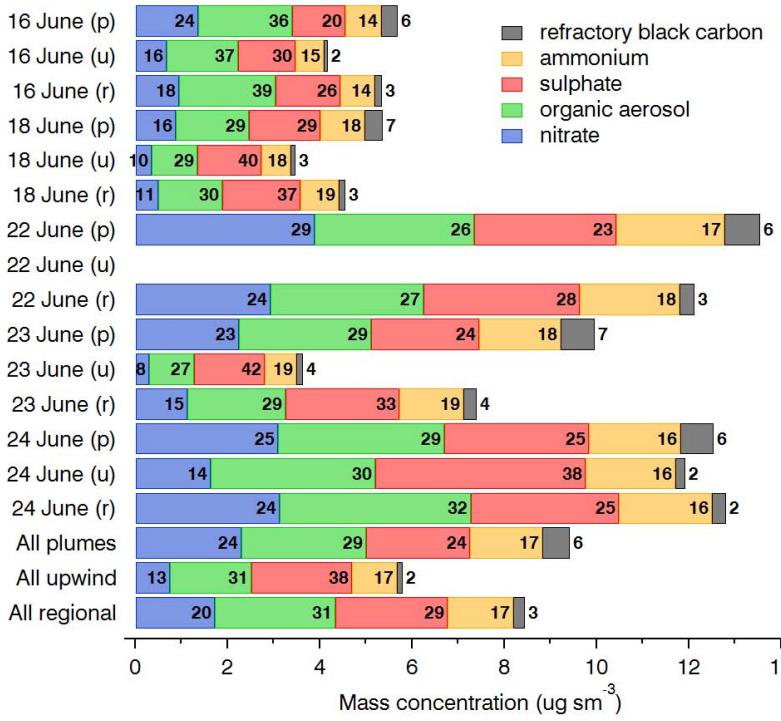

Fig. 10. Mass concentrations of AMS- and SP2-measured species averaged over London plume (p), upwind of London segments (u) and regional segments (r) for each flight as well as the campaign-averaged values for each category. Black numbers indicate the mass fraction (%) of each species relative to the corresponding total sub-micron mass.

sub-micron mass/ΔCO ratios with photochemical age. The regression of SSA on photochemical age yielded an increase of $0.0013\pm0.0002\,h^{-1}$, but there was considerable variability ($r^2 = 0.25$). The total sub-micron mass measured by the AMS normalized by rBC increased from roughly $10\,g\,g^{-1}$ BC to as much as $50\,g\,g^{-1}$ BC after 40 h, with an average increase of $0.34\pm0.05\,h^{-1}$ ($r^2 = 0.33$).

The addition of secondary material and coagulation processes can lead to changes in the rBC mixing state and coating thickness (Moteki et al., 2007; Schwarz et al., 2008; Subramanian et al., 2010), so we compared one measure of rBC mixing state, the number fraction of "thickly coated" particles to photochemical age. The number fraction of "thickly coated" particles increased from approximately 0.18 at $t = 0$ to a maximum of approximately 0.3 at $t = 45$ h, but there was considerable variability in the data. The average increase was approximately $0.08\,\%\,h^{-1}$, significantly lower than $2.3\,\%\,h^{-1}$ reported by Moteki et al. (2007). Subramanian et al. (2010) also calculated rates of increase in the thickly coated fraction of $0.2–0.25\,\%\,h^{-1}$ over and downwind of Mexico City, closer to our reported values. One important distinction between our results and those reported by Moteki et al. (2007) and Subramanian et al. (2010) in addition to differences in aerosol and photochemical environment was that we considered the entire rBC population but the previous studies restricted their analyses of the conversion rate to thickly coated rBC to particles within a specific mass/size range. There was no evidence of observed changes in rBC mixing state with time causing higher mass absorption efficiencies, which might be expected (Bond et al., 2006). This may have been due to different rBC sources to the plume and non-plume regions sampled, measurement artefacts associated with the PSAP light absorption measurement, or changes in rBC structure. See McMeeking et al. (2011) for a more detailed discussion.

3.4 Aerosol chemical properties

The sub-micron aerosol mass concentrations for the major chemical components are summarized for all flights in Fig. 10 and details for specific circuits are shown in Fig. 11. Total sub-micron mass (calculated from the total mass of aerosol measured by the AMS plus rBC measured by the SP2) was relatively homogeneous around the circuit for all flights. On average, the sub-micron aerosol mass concentrations were about 12 % higher in the plume compared to the regional air and for individual flights were higher than regional values for all but the 24 June flight. Mass concentrations were between 4–8 $\mu g\,sm^{-3}$ for the 16 and 18 June flights and between 8–20 $\mu g\,sm^{-3}$, for the 22–24 June flights. The higher aerosol mass loadings on the 22–24 June flights resulted from transport of pollution from continental Europe, consistent with the elevated CO mixing ratios also observed.

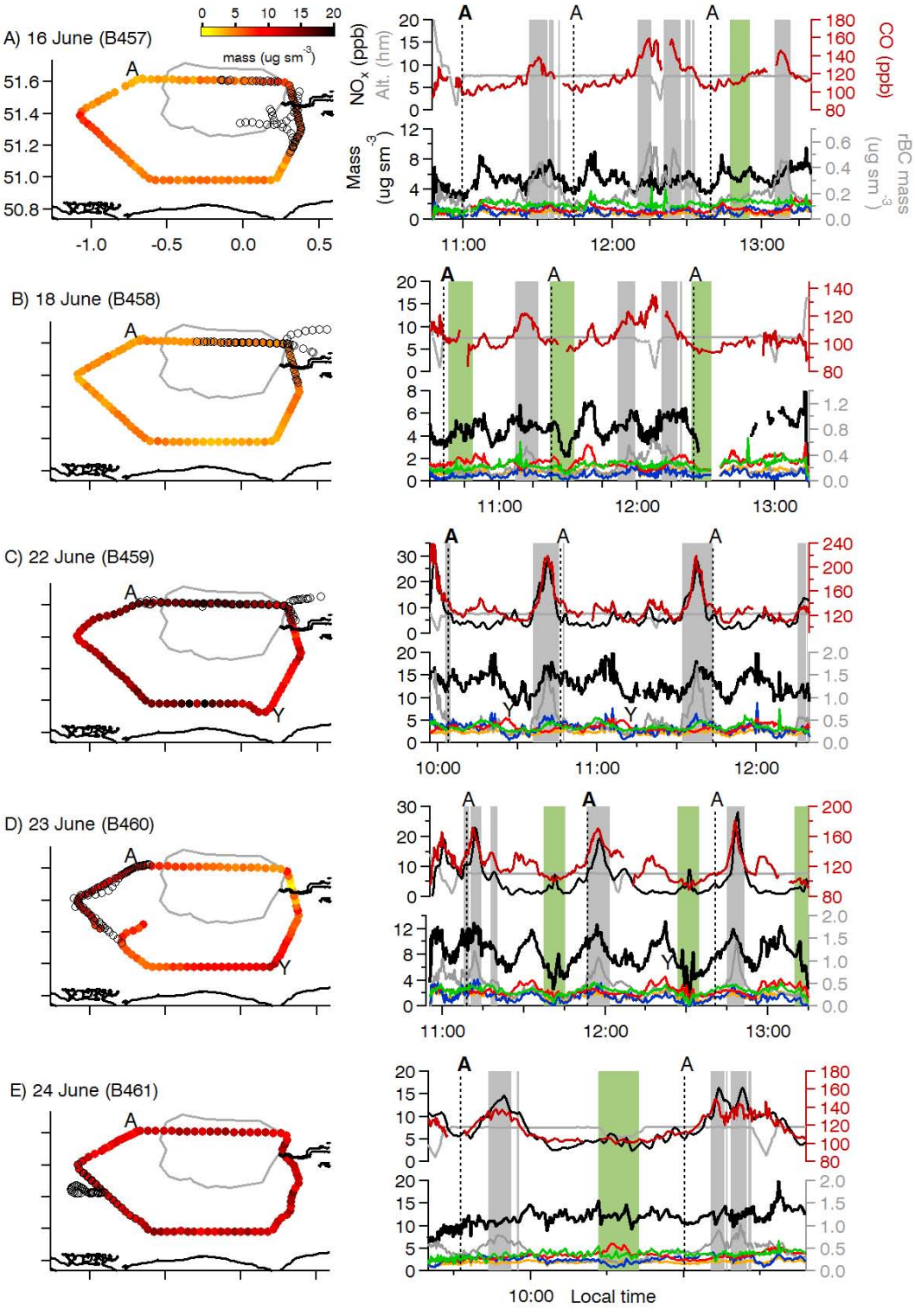

Fig. 11. Examples of aerosol sub-micron mass concentrations measured during a single circuit around London for each flight. Also shown are time series for altitude (grey), nitrogen oxides (black), carbon monoxide (red), aerosol sulphate (red), nitrate (blue), organics (green), ammonium (orange), and refractory black carbon (grey) measured by the AMS and SP2. The time series are restricted to periods when the aircraft was flying circuits around London. Shaded regions and outlined circles indicate regions identified as either in plume or upwind based on air mass classification method described in the text.

Table 4. Average OA/ΔCO, rBC/ΔCO, single scattering albedo (SSA) and mass absorption efficiency (MAE) for plume and non-plume periods determined from the photochemical age calculated from whole air canister toluene and benzene mixing ratios. Only flights with valid canister data are listed.

Date	Flight ID	OA/ΔCO [μg sm^{-3} ppmv^{-1}]	rBC/ΔCO [ng sm^{-3} ppbv^{-1}]	SSA	MAE [m^2 g^{-1}]	# samples
Plumes (t_{photo} <20 h)						
18 June	B458	13	13.1	0.86	6.0	2
21 June	B459	6.8±6.5	8.6±2.0	0.88±0.03	11.6±1.5	6
22 June	B460	8.1±3.2	12.0±1.8	0.84±0.03	9.1±0.8	12
	Average	9.3±3.3	11.2±2.3	0.86±0.02	8.9±2.8	20
Non-plume/background (t_{photo} >50 h)						
18 June	B458	54±11	11.0±1.5	0.93±0.03	9.2±1.9	17
21 June	B459	30±19	10.3±1.9	0.94±0.007	3.7±2	5
22 June	B460	64±9	9.3±0.8	0.86±0.04	5.9±8.4	8
	Average	49±17	10.2±0.9	0.91±0.04	6.3±2.8	30

The lowest aerosol mass concentrations occurred on 18 June during a period of strong westerly flow following passage of a cold front.

Averaged over the campaign the aerosol in the London plume had roughly equal contributions from nitrate, OA and sulphate with lower contributions from ammonium and rBC. The average contributions from each species to total sub-micron mass in the London plume were approximately 6 % for rBC, 24 % for nitrate, 17 % for ammonium, 24 % for sulphate, and 29 % for OA. The regional air masses had slightly higher contributions from OA and sulphate and less nitrate (3 % for rBC, 20 % for nitrate, 17 % for ammonium, 29 % for sulphate, and 31 % for OA). Aerosol sampled upwind of London had less nitrate and rBC and a stronger relative contribution from sulphate. The enhancement of nitrate aerosol in the urban plume was also evident in the positive correlation between nitrate-sulphate ratios and rBC around the circuits ($r^2 = 0.42$). We normalized by sulphate mass to account for regional contributions to nitrate in the plume, on the basis that urban sulphate precursor emissions in London are minor compared to nitrate precursor emissions according to the LAEI. The increase in nitrate could have resulted from the new formation of nitric acid via oxidation of nitrogen oxides emitted by the city and combination with urban ammonia emissions or pre-existing agricultural emissions upwind to form ammonium nitrate. In addition, it is possible that re-partitioning of nitrate from super-micron particles that are not detected by the AMS to detectable sub-micron particles was responsible for some of the observed increase. Super-micron/coarse mode nitrate arises from the surface reaction of nitric acid on sea salt aerosol. The lack of a significant super-micron contribution to aerosol volume suggests that re-partitioning is the less likely explanation, but we do not rule out either possibility.

Dall'Osto et al. (2009) identified two types of nitrate in London using a single particle aerosol mass spectrometer: a "local" nitrate formed in the urban area during the night and a larger-sized "regionally transported" nitrate. Our airborne measurements support both a strong regional contribution to nitrate, evident in the relatively high non-plume legs of the flights, as well as a local contribution. The "local" nitrate source was evident in our daytime measurements because of the lower temperatures and higher relative humidity aloft, discussed in more detail in Sect. 3.5. Thus, while Dall'Osto et al. (2009) observed a disappearance of the local nitrate during the day that they attributed to increased temperature (resulting in volatilization), decreased relative humidity and changes in the boundary layer depth, we still observed a minor, local source of nitrate from the city. Despite the increase in nitrate, total sub-micron aerosol mass concentrations increased either only slightly or in one case (24 June) decreased in the plume, indicating that sub-micron PM emissions from the city were still minor (15 %) compared to contributions from regional aerosol. Refractory black carbon mass concentrations increased by more than a factor of two in the plume, but only represented a small contribution to sub-micron aerosol mass.

Aerosol composition has been previously measured by an AMS over and in the outflow of several major cities (de Gouw and Jimenez, 2009), including Mexico City (DeCarlo et al., 2008). Mexico City is a much larger urban region than London and is confined by topography and influenced by a number of additional sources including wildfires and volcanoes (DeCarlo et al., 2008; Yokelson et al., 2007). Its lower latitude and higher altitude compared to London means more radiation is available for photochemical reactions. DeCarlo et al. (2008) observed average AMS mass concentrations of 26.6 μg sm^{-3} in the Mexico City basin, of which about 60 % was OA, 23 % nitrate and 7 % by sulphate. The higher average OA mass fraction in Mexico City compared to London (60 % versus 30 %) was not surprising given the large differences in photochemical environments and emissions.

Finer-scale changes in aerosol and trace gas concentrations are shown in Fig. 11, which gives total aerosol concentrations along the flight track for a single circuit around London and time series for periods when the aircraft was flying the circuits. We observed elevated sulphate concentrations in several locations around the circuit for multiple flights, particularly during the southern legs (e.g., points Y on Fig. 10c and d). The higher sulphate concentrations observed at point Y on 18 June coincided with elevated sulphur dioxide concentrations (not shown) and the transport predicted from the UK4 model suggested these were emissions from the Southampton area, possibly shipping and/or power-plants. The mean, low-level flow on the 23 and 24 June flights and backward trajectory analysis (not shown) indicated that on these occasions the elevated sulphate concentrations likely resulted from transport from continental Europe, particularly the Netherlands and Belgium regions. Carbon monoxide, NO_x (available 22–24 June only) and rBC were strongly correlated and increased during the London plume intercepts, which are shaded in Fig. 11. As noted previously, there was little change in total aerosol mass concentrations, with only minor increases in nitrate and to a lesser degree organics during plume intercepts compared to regions outside the plume.

Aerosol mass concentrations are often normalized by gas-phase tracers of different emission sources to aid comparisons between measurement locations while accounting for the effects of dilution on absolute concentrations. Increases in the aerosol species relative to a long-lived tracer such as CO reflect secondary production, assuming a constant emission ratio. We examined relationships between aerosol species and trace gas mixing ratios for a subset of three flights (18, 22 and 23 June) with valid gas-phase data from whole air canister samples. Nitrate was positively correlated with ΔCO, acetylene and other traffic-related VOCs with significantly different relationships inside and outside of the London plume. The average non-plume (photochemical age >50 h) nitrate/ΔCO ratio was $80\,\mu g\,sm^{-3}\,ppmv^{-1}$ ($r^2 = 0.69$) compared to $20–30\,\mu g\,sm^{-3}\,ppmv^{-1}$ in the plumes (photochemical age <20 h), reflecting the enhancement of nitrate relative to ΔCO in aged, regional pollution. Note here we rely on gas-phase data to distinguish between the plume and non-plume samples rather than the rBC data available for all five flights. Our observations differ from observations of decreases in nitrate-ΔCO ratios downwind of Mexcio Cit by DeCarlo et al. (2008), which may have resulted from dilution with air with low concentrations of nitric acid and/or ammonia. We lacked the gas-phase measurements of these compounds needed to explore possible reasons for the differences in nitrate-ΔCO ratios,but suspect stronger regional-contributions to NO_x and ammonia over north-western Europe combined with our inability to sample the aged London emissions are responsible.

OA was also positively correlated with ΔCO ($r^2 = 0.50$) and had different relationships inside and outside of the London plume. The average OA/ΔCO ratio for photochemical age >50 h was $\sim 45\,\mu g\,sm^{-3}\,ppmv^{-1}$ but lower ($\sim 10\,\mu g\,sm^{-3}\,ppmv^{-1}$) during plume sampling (Table 4). The relationships between nitrate and OA mass concentrations with respect to acetylene, ethane and other long-lived VOCs also showed similar relationships as those observed for ΔCO. Allan et al. (2010) measured OA and CO in central London and calculated an average OA/ΔCO ratio of $10.30\,\mu g\,sm^{-3}\,ppmv^{-1}$ using linear regression. They restricted their calculation to sub-200 nm diameter OA, but our size-resolved OA data for the circuit flights was too variable to allow a similar calculation. Our observed OA/ΔCO ratio of $\sim 10\,\mu g\,sm^{-3}\,ppmv^{-1}$ in the London plume was similar to the Allan et al. (2010) value despite the larger size range of OA in our calculations. We suspect the addition of OA mass for diameter >200 nm particles in our calculation was offset by different source footprints. We observed much lower OA/ΔCO ratios in the London plume compared to a value of approximately $80\,\mu g\,sm^{-3}\,ppmv^{-1}$ measured in the Mexico City outflow by DeCarlo et al. (2008). DeCarlo et al. (2008) attributed the high OA/ΔCO ratio to a combination of rapid photochemistry and biomass burning influence. The production of secondary OA in urban plumes means that OA/ΔCO ratios increase with age. Several studies showed clear increases in OA/ΔCO from approximately 10 to $80\,\mu g\,sm^{-3}\,ppmv^{-1}$ in aging emissions from Mexico city (DeCarlo et al., 2010; Dzepina et al., 2009; Kleinman et al., 2008). Our observations of higher OAΔCO in the regional pollution outside of the London plume are consistent with the previous observations if we assume that dominant source of OA and CO in the study region originates from urban centres with similar initial OA/ΔCO Photochemical reactions likely proceeded more slowly over London compared to Mexico City due to lower trace gas concentrations and reduced actinic flux. de Gouw and Jimenez (2009) summarized recent AMS OA measurements for urban emissions and reported that primary OA/ΔCO ratios were typically between 5-15 $\mu g\,sm^{-3}\,ppmv^{-1}$, in agreement with our London plume measurements. They suspected the lower end of this range was more accurate due to the difficulty in accounting for the rapid formation of SOA and background SOA downwind of urban sources. de Gouw and Jimenez (2009) also examined aged urban air and found that OA/ΔCO ratios were about $70\pm20\,\mu g\,sm^{-3}\,ppmv^{-1}$ for a wide range of emissions and photochemical environments. Our measured OA/ΔCO ratios in non-plume air around London were also consistent with these results, providing further evidence of the important contributions by SOA, even in regions with large urban emission sources such as north western Europe. We stress that our non-plume and plume sampling did not measure the same air mass or sources, but rather represent the contrast between emissions from a major European megacity (London) with surrounding regional pollution from a variety of UK and European sources.

Refractory BC is a combustion product produced by vehicle traffic, so we compared its measured mass concentrations to other traffic tracers including CO and certain VOCs. Several previous studies have examined BC/ΔCO relationships and have reported values ranging from ∼1–6 ng sm^{-3} ppbv^{-1} (Baumgardner et al., 2007; McMeeking et al., 2010; Spackman et al., 2008; Subramanian et al., 2010). Using whole air canister samples, we observed substantially higher ratios downwind of London, with rBC/ΔCO approximately 10–12 ng sm^{-3} ppbv^{-1}. Refractory BC/ΔCO ratios reflect the mix of sources within the city, and for London we believe the increased contributions from diesel vehicles, which produce relatively more rBC compared to petrol vehicles, explain the higher rBC/ΔCO ratios compared to other locations. Refractory BC was also correlated with other traffic-related and relatively long-lived VOCs, including ethane ($r^2 = 0.72$) and acetylene ($r^2 = 0.81$).

3.5 Aerosol vertical structure

Each research flight included vertical profiles from approximately 3000 m to the surface before the first circuit around London in the vicinity of Northolt airfield (Fig. 1). Each profile occurred at approximately 10:00 UTC ±1 h. Potential temperature, potential dew point temperature and aerosol mass concentrations for individual species measured by the AMS and rBC during the profiles are shown in Fig. 12. The planetary boundary layer (PBL) height was about 1900 m for the 16 and 18 June flights. Two distinct layers were visible on the 22 June flight, with a well-mixed layer (constant potential temperature) extending from the surface to approximately 1200 m underneath a warmer (in terms of potential temperature) layer extending up to 2100 m. The upper layer was no longer evident by the 23 June and the mixed layer extended from the surface up to approximately 1400 m. The feature was also apparent during the 24 June flight, with a shallow mixed layer extending from the surface up to 750 m underneath a warmer, deeper layer extending up to 1900 m.

The mass concentrations during the two westerly flights (16 and 18 June) were lower throughout the depth of the PBL compared to the 22–24 June flights. The profiles revealed a more complicated vertical structure for the flights where anti-cyclonic conditions dominated on 22–24 June. Within the PBL, nitrate mass concentrations increased with altitude, as previously observed by Morgan et al. (2009) during similar airborne measurements over the UK. They linked the enhancement of nitrate with altitude to decreases in temperature and increases in RH that altered the equilibrium of the nitric acid-ammonia-ammonium nitrate system towards the particle/ammonium nitrate phase. This is consistent with the increase in nitrate with relative humidity observed during several flights around London. For example, during the 23 June flight (B460), nitrate mass concentrations increased by a factor of 3 for a 40 % increase in RH whereas sulphate and OA concentrations remained constant. Previous

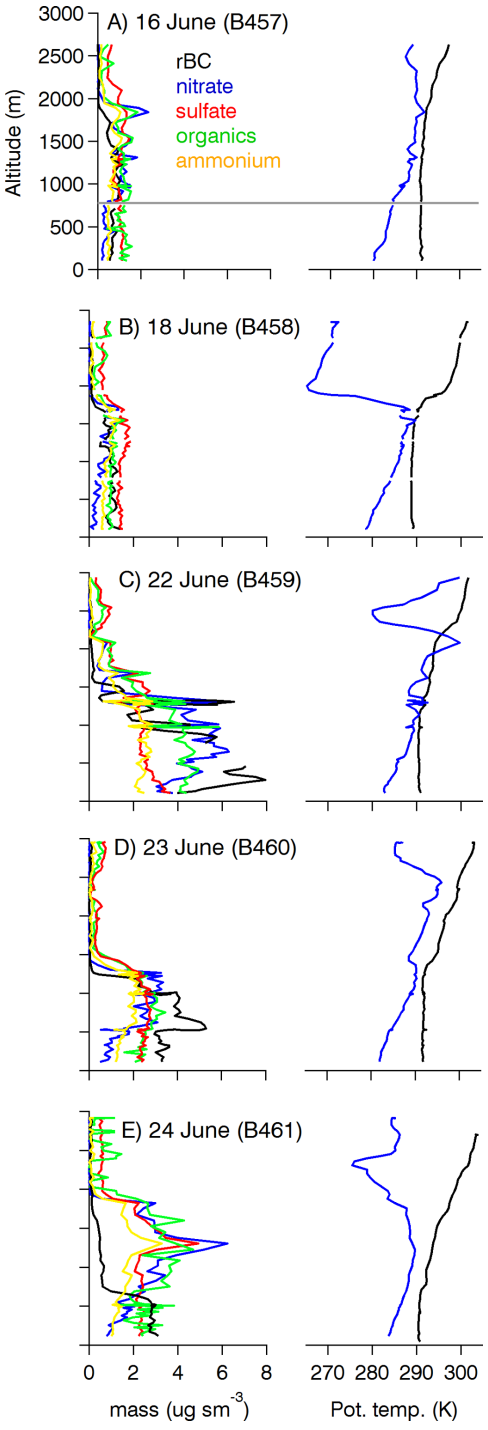

Fig. 12. Altitude profiles in the vicinity of Northolt airfield (Fig. 1) for (left) sub-micron aerosol mass concentrations over London and (right) potential temperature (black) and potential dew point temperature (blue). Refractory black carbon (rBC) was measured by the SP2 and organics, nitrate, sulphate and ammonium were measured by the AMS. rBC mass concentrations were multiplied by five to appear on the same scale as the AMS species. The horizontal grey line shows the altitude of the around London circuits. All axes are to identical scales.

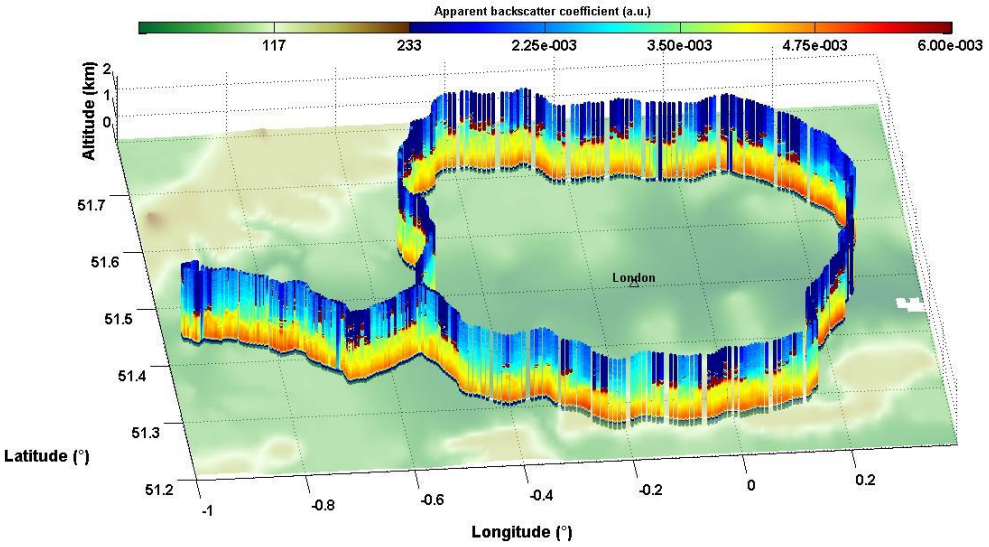

Fig. 13. Apparent lidar backscatter coefficient at 355 nm measured around the M25 motorway on the 16 June.

field (Neuman et al., 2003) and modelling studies (Morino et al., 2006) have also observed increases in the fraction of nitrate in the particle phase over urban centres that were associated with decreases in temperature and increases in relative humidity. Mass concentrations of rBC indicated a more highly polluted layer close to the surface for the 23 and 24 June flights, which corresponded to the shallower, dryer mixed layer. McMeeking et al. (2011) discuss several aspects of the vertical structure of rBC mass concentrations and their physical properties in more detail.

Morgan et al. (2009) also performed a statistical analysis of aerosol composition measured by an AMS from the FAAM research aircraft for more than 300 profiles around the UK coastline. They used a cluster analysis technique to group profiles according to air mass trajectory, which included an Atlantic or westerly cluster, an easterly cluster and a stagnant or low transport cluster. Aerosol concentrations (and nitrate in particular) were generally lower for the Atlantic cluster compared to the easterly and stagnant clusters. Our observations around London show similar results for aerosol concentrations and composition. The two westerly flights (16 and 18 June) feature lower aerosol concentrations compared to the easterly and stagnant cases (22–24 June), with lower nitrate concentrations observed during profiles. Nitrate mass concentrations increased approximately four-fold during profiles in easterly and stagnant conditions compared to westerly, also consistent with the findings of Morgan et al. (2009). Sub-micron mass concentrations during the easterly cases were slightly higher than the 75th percentile values reported by Morgan et al. (2009), meaning conditions during these flights (22–24 June) represented relatively polluted conditions for the UK, consistent with the ground-based $PM_{2.5}$ statistics (Fig. 3).

The aerosol vertical structure was also probed by the mobile, van-based lidar system, which operated on selected days during the campaign. A separate analysis focuses in detail on the ground-based lidar and on comparisons between the ground-based lidar and aircraft measurements during the campaign and we only include a brief description of some basic results here. Figure 13 presents an example of a lidar "curtain" measured around the M25 on the same day as flight B457 (16 June). The lidar signals have been calibrated, range-corrected, corrected from the overlap factor and for molecular transmission (Chazette, 2003). We compared the aircraft-measured ambient extinction coefficients individual aircraft profiles between 0–3 km to lidar-retrieved extinction coefficients averaged over regions in close proximity to the location of the aircraft measurements. The PSAP time resolution was too slow to measure light absorption coefficients directly, so we estimated them from the SP2 rBC mass concentrations, using flight-average MAE values to convert to light absorption coefficients. Figure 14 shows profile data for two flight days, 16 and 23 June, where the presence of clouds did not interfere with the lidar retrievals. We also show altitude-averaged aerosol composition data measured by the AMS and SP2 during each profile. The profile patterns were flown roughly upwind (northwest for 16 June and east for 23 June) and downwind (northeast for 16 June and northwest for 23 June) of central London. It should be stressed that the aircraft profiles do not represent a perfectly vertical column of the atmosphere, but are spread out in horizontal space as well due to the restrictions on the aircraft flight path. Small scale horizontal features, including plumes, can appear to be a vertical feature for this reason, so some care should be used in interpreting the profile measurements.

The aircraft and lidar measurements showed qualitatively similar results for both flight days and in both the upwind

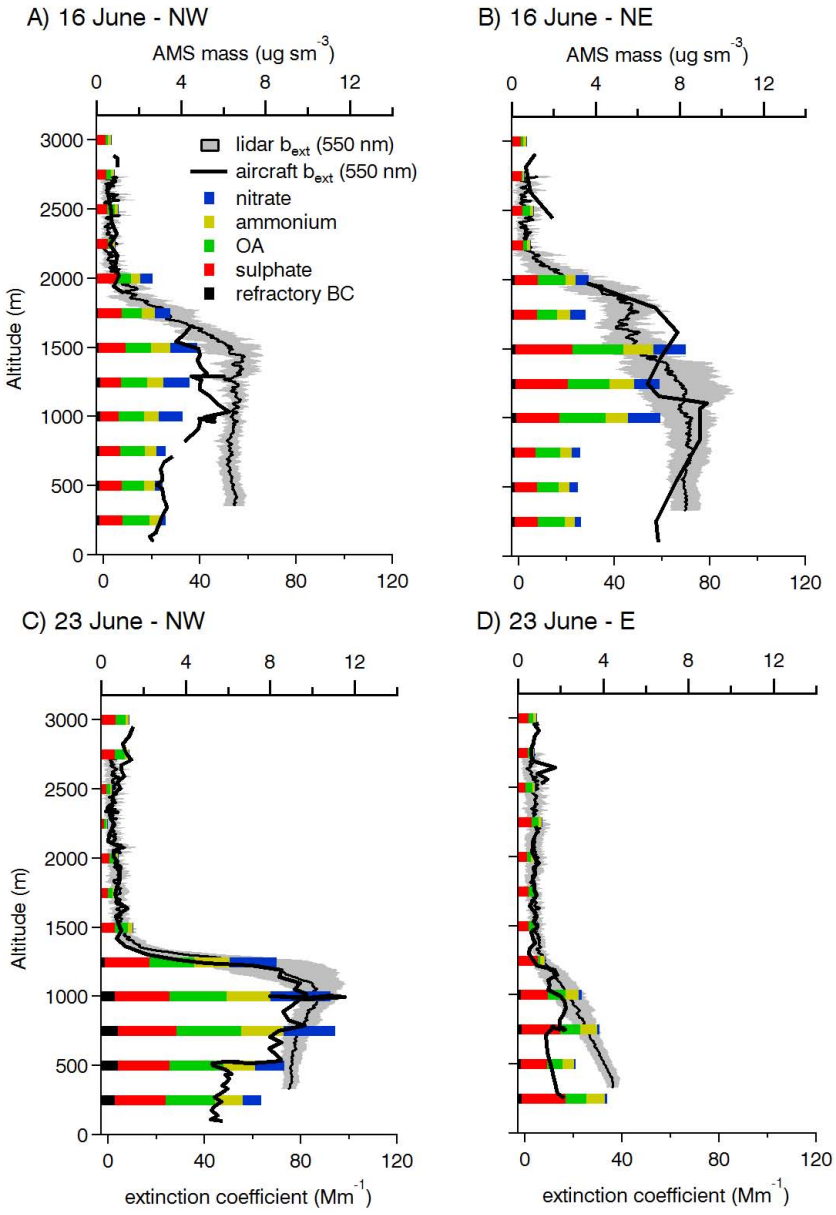

Fig. 14. Aircraft measured aerosol composition (averaged over 250 m thick altitude bins, coloured bars) and extinction coefficients (thick black lines) for individual profile segments flown to the **(a)** northwest and **(b)** northeast of central London on 16 June and **(c)** northwest and **(d)** east of central London on 23 June. Average light extinction coefficients (thin black lines) retrieved from van-based lidar measurements in the vicinity of the aircraft profiles and their variance expressed as a root mean square (shaded grey region) are also shown.

and downwind regions. The 16 June profiles showed a deeper mixed layer extending to approximately 1.5 km and the 23 June profiles showed a shallower mixed layer extending to approximately 1.2 km. The upwind profiles were lower compared to the downwind profiles in terms of aircraft measured scattering coefficients, aerosol mass and lidar-measured extinction coefficients. Lidar- and aircraft-measured extinction coefficients were in relatively good agreement, particularly at higher altitudes and showed similar vertical structure. The discrepancies between aircraft- and lidar-measured values are likely due to modification of the aerosol when it was sampled into the aircraft, such as the loss of coarse mode particles and semi-volatile material, errors in the assumed optical properties needed to convert the lidar backscatter measurements at 355 nm to light extinction coefficients at 550 nm, and deviations from the assumed f(RH) and MAE needed to reconstruct extinction coefficients from the PSAP and nephelometer aircraft measurements.

4 Conclusions

We carried out a series of research flights and ground-based lidar van circuits around the mega-city of London. The London plume could be distinguished from a regional background by higher concentrations of major vehicle traffic emission tracers, including CO, NO_x, certain VOCs and rBC. Total sub-micron aerosol mass concentrations increased on average by approximately 12 % in the plume, in contrast to the large differences in gas-phase compounds and rBC observed in and out of the plume. The small difference in aerosol concentrations in the London plume versus the region outside the plume indicates that regional sources are still important, at least for the conditions we sampled. The aerosol surrounding London may be driven more by factors governing regional aerosol concentrations and composition rather than on the London urban source. We stress that the measurements of London emissions were made in air masses dominated by fresher emissions compared to the regional samples, and therefore may represent a lower limit due to the expected secondary production of additional, primarily OA, mass. Refractory black carbon mass concentrations roughly doubled in the plume, but they were a small contributor to total sub-micron mass and most of the observed increases resulted from higher nitrate concentrations. Despite its relatively small influence on sub-micron mass, rBC emitted by London reduced the aerosol single scattering albedo (plume average of 0.86 versus 0.91 for the regional aerosol), which may have important regional climate effects. Organic aerosol to carbon monoxide ratios observed in the plume ($10\,\mu g\,sm^{-3}\,ppmv^{-1}$) and in regional aerosol ($45\,\mu g\,sm^{-3}\,ppmv^{-1}$) were similar to other recently reported measurements for urban emissions and regional/aged pollution. VOC emission ratios in London were also similar to those measured downwind of major US cities. Comparisons between aircraft-measured profiles and lidar retrieved aerosol showed similar vertical structure.

Acknowledgements. The EM25 campaign was supported by the UK Met Office and the Natural Environment Research Council (NERC) APPRAISE-ADIENT project (NE/E-011101/1). The mobile lidar van was supported by the Commissariat à l'Energie Atomique (CEA). Airborne data were obtained using the BAe-146-301 Atmospheric Research Aircraft (ARA) flown by Directflight Ltd. and managed by the Facility for Airborne Atmospheric Measurements (FAAM), which is a joint entity of the Natural Environment Research Council (NERC) and the Met Office. We thank the FAAM, Directflight and Avalon project partners for their support during the campaign and the FAAM pilots in particular for safely negotiating the busy London airspace. London air quality ground stations are supported by the Environmental Research Group at Kings College London and the Automatic Hydrocarbons Monitoring Network are supported by the Department for Environment, Food and Rural Affairs (DEFRA). We also thank P. I. Williams, G. Capes and M. Flynn for AMS and SP2 instrument support. The NERC National Centre for Atmospheric Sciences supported maintenance of the AMS, the Whole Air Sampling system and the off-line GC analyses. ECMWF reanalysis data were provided by the ERA-Interim data extraction tool. We also thank D. Baumgardner and an anonymous reviewer for their comments.

Edited by: B. Ervens

References

Aiken, A. C., Salcedo, D., Cubison, M. J., Huffman, J. A., Decarlo, P. F., Ulbrich, I. M., Docherty, K. S., Sueper, D., Kimmel, J. R., Worsnop, D. R., Trimborn, A., Northway, M., Stone, E. A., Schauer, J. J., Volkamer, R. M., Fortner, E., de Foy, B., Wang, J., Laskin, A., Shutthanandan, V., Zheng, J., Zhang, R., Gaffney, J., Marley, N. A., Paredes-Miranda, G., Arnott, W. P., Molina, L. T., Sosa, G., and Jimenez, J. L.: Mexico City aerosol analysis during MILAGRO using high resolution aerosol mass spectrometry at the urban supersite (T_0) – Part 1: Fine particle composition and organic source apportionment, Atmos. Chem. Phys., 9, 6633–6653, doi:10.5194/acp-9-6633-2009, 2009.

Allan, J. D., Williams, P. I., Morgan, W. T., Martin, C. L., Flynn, M. J., Lee, J., Nemitz, E., Phillips, G. J., Gallagher, M. W., and Coe, H.: Contributions from transport, solid fuel burning and cooking to primary organic aerosols in two UK cities, Atmos. Chem. Phys., 10, 647–668, doi:10.5194/acp-10-647-2010, 2010.

Allen, G., Coe, H., Clarke, A., Bretherton, C., Wood, R., Abel, S. J., Barrett, P., Brown, P., George, R., Freitag, S., McNaughton, C., Howell, S., Shank, L., Kapustin, V., Brekhovskikh, V., Kleinman, L., Lee, Y.-N., Springston, S., Toniazzo, T., Krejci, R., Fochesatto, J., Shaw, G., Krecl, P., Brooks, B., McMeeking, G., Bower, K. N., Williams, P. I., Crosier, J., Crawford, I., Connolly, P., Allan, J. D., Covert, D., Bandy, A. R., Russell, L. M., Trembath, J., Bart, M., McQuaid, J. B., Wang, J., and Chand, D.: South East Pacific atmospheric composition and variability sampled along 20° S during VOCALS-REx, Atmos. Chem. Phys., 11, 5237-5262, doi:10.5194/acp-11-5237-2011, 2011.

Anderson, T. L., Covert, D. S., Marshall, S. F., Laucks, M. L., Charlson, R. J., Waggoner, A. P., Ogren, J. A., Caldow, R., Holm, R. L., Quant, F. R., Sem, G. J., Wiedensohler, A., Ahlquist, N. A., and Bates, T. S.: Performance characteristics of a high-sensitivity, three-wavelength, total scatter/backscatter nephelometer, J. Atmos. Ocean. Technol., 13, 967–986, 1996.

Anderson, T. L. and Ogren, J. A.: Determining Aerosol Radiative Properties Using the TSI 3563 Integrating Nephelometer, Aerosol Sci. Technol., 29, 57–69, doi:10.1080/02786829808965551, 1998.

Atkinson, R.: Atmospheric chemistry of VOCs and NO_x, Atmos. Environ., 34, 2063–2101, doi:10.1016/S1352-2310(99)00460-4, 2000.

Atkinson, R. W., Barratt, B., Armstrong, B., Anderson, H. R., Beevers, S. D., Mudway, I. S., Green, D., Derwent, R. G., Wilkinson, P., and Tonne, C.: The impact of the congestion charging scheme on ambient air pollution concentrations in London, Atmos. Environ., 43, 5493–5500, doi:10.1016/j.atmosenv.2009.07.023, 2009.

Banta, R. M., Senff, C. J., Nielsen-Gammon, J., Darby, L. S., Ryerson, T. B., Alvarez, R. J., Sandberg, S. P., Williams, E. J., and Trainer, M.: A Bad Air Day in Houston, B. Am. Meteorol. Soc., 86, 657, doi:10.1175/BAMS-86-5-657, 2005.

Baumgardner, D., Kok, G. L., and Raga, G. B.: On the diurnal variability of particle properties related to light absorbing carbon in Mexico City, Atmos. Chem. Phys., 7, 2517–2526, doi:10.5194/acp-7-2517-2007, 2007.

Baumgardner, D., Kok, G., and Raga, G.: Warming of the Arctic lower stratosphere by light absorbing particles, Geophys. Res. Lett., 31, L06117, doi:10.1029/2003GL018883, 2004.

Bigi, A. and Harrison, R. M.: Analysis of the air pollution climate at a central urban background site, Atmos. Environ., 44, 2004–2012, doi:10.1016/j.atmosenv.2010.02.028, 2010.

Bond, C. M., Anderson, T. L., Campbell, D., and Bond, T. C.: Calibration and intercomparison of filter-based measurements of visible light absorption by aerosols, Aerosol Sci. Technol., 30, 582–600, 1999.

Bond, T. C., Habib, G. and Bergstrom, R. W.: Limitations in the enhancement of visible light absorption due to mixing state, J. Geophys. Res., 111, D20211, doi:10.1029/2006JD007315, 2006.

Bond, T. and Bergstrom, R.: Light Absorption by Carbonaceous Particles: An Investigative Review, Aerosol Sci. Technol., 40, 27–67, doi:10.1080/02786820500421521, 2006.

Canagaratna, M. R., Jayne, J. T., Jimenez, J. L., Allan, J. D., Alfarra, M. R., Zhang, Q., Onasch, T. B., Drewnick, F., Coe, H., Middlebrook, A., Delia, A., Williams, L. R., Trimborn, A. M., Northway, M. J., DeCarlo, P. F., Kolb, C. E., Davidovits, P., and Worsnop, D. R.: Chemical and microphysical characterization of ambient aerosols with the aerodyne aerosol mass spectrometer, Mass Spectrom. Rev., 26, 185–222, doi:10.1002/mas.20115, 2007.

Cappa, C. D., Lack, D. A., Burkholder, J. B., and Ravishankara, A. R.: Bias in filter-based aerosol light absorption measurements due to organic aerosol loading: Evidence from laboratory measurements, Aerosol Sci. Technol., 42, 1022–1032, doi:10.1080/02786820802389285, 2008.

Chazette, P.: The monsoon aerosol extinction properties at Goa during INDOEX as measured with lidar, J. Geophys. Res., 108, 4187, doi:10.1029/2002JD002074, 2003.

Chazette, P., Randriamiarisoa, H., Sanak, J., and Couvert, P.: Optical properties of urban aerosol from airborne and ground-based in situ measurements performed during the Etude et Simulation de la Qualité de l'air en Ile de France (ESQUIF) program, J. Geophys. Res., 110, D02206, doi:10.1029/2004JD004810, 2005.

Chazette, P., Sanak, J., and Dulac, F.: New approach for aerosol profiling with a Lidar onboard an ultralight aircraft: Application to the African Monsoon Multidisciplinary Analysis, Environ. Sci. Technol., 41, 8335–8341, 2007.

Chazette, P., Raut, J.-C., Dulac, F., Berthier, S., Kim, S-W, Royer, P., Sanak, J., Loaec, S., and Grigaut-Desbrosses, H.: Simultaneous observations of lower tropospheric continental aerosols with a ground-based, an airborne and the spaceborne CALIOP lidar systems, J. Geophys. Res., 115, D00H31, doi:10.1029/2009JD012341, 2010.

Chazette, P., Bocquet, M., Royer, P., Winiarek, V., Raut, J.-C., Labazuy, P., Gouhier, M., Lardier, M., and Cariou, J.-P.: Eyjafjallajökull ash concentrations derived from both lidar and modeling, J. Geophys. Res., 117, D00U14, doi:10.1029/2011JD015755, 2012.

Clark, P. A., Harcourt, S. A., Macpherson, B., Mathison, C. T., Cusack, S., and Naylor, M.: Prediction of visibility and aerosol within the operational Met Office Unified Model. I?: Model formulation and variational assimilation, Q. J. Roy. Meteorol. Soc., 134, 1801–1816, doi:10.1002/qj.318, 2008.

Dall'Osto, M., Harrison, R. M., Coe, H., Williams, P. I., and Allan, J. D.: Real time chemical characterization of local and regional nitrate aerosols, Atmos. Chem. Phys., 9, 3709–3720, doi:10.5194/acp-9-3709-2009, 2009.

Davies, L., Bell, J. N. B., Bone, J., Head, M., Hill, L., Howard, C., Hobbs, S. J., Jones, D. T., Power, S. a, Rose, N., Ryder, C., Seed, L., Stevens, G., Toumi, R., Voulvoulis, N., and White, P. C. L.: Open Air Laboratories (OPAL): A community-driven research programme, Environmental Pollution, 159, 2203–2210, doi:10.1016/j.envpol.2011.02.053, 2011.

DeCarlo, P. F., Dunlea, E. J., Kimmel, J. R., Aiken, A. C., Sueper, D., Crounse, J., Wennberg, P. O., Emmons, L., Shinozuka, Y., Clarke, A., Zhou, J., Tomlinson, J., Collins, D. R., Knapp, D., Weinheimer, A. J., Montzka, D. D., Campos, T., and Jimenez, J. L.: Fast airborne aerosol size and chemistry measurements above Mexico City and Central Mexico during the MILAGRO campaign, Atmos. Chem. Phys., 8, 4027–4048, doi:10.5194/acp-8-4027-2008, 2008.

DeCarlo, P. F., Ulbrich, I. M., Crounse, J., de Foy, B., Dunlea, E. J., Aiken, A. C., Knapp, D., Weinheimer, A. J., Campos, T., Wennberg, P. O., and Jimenez, J. L.: Investigation of the sources and processing of organic aerosol over the Central Mexican Pleateau from aircraft measurements during MILAGRO, Atmos. Chem. Phys., 10, 5257–5280, doi:10.5194/acp-10-5257-2010, 2010.

Dollard, G. J., Dumitrean, P., Telling, S., Dixon, J. and Derwent, R. G.: Observed trends in ambient concentrations of C2–C8 hydrocarbons in the United Kingdom over the period from 1993 to 2004, Atmos. Environ., 41, 2559–2569, doi:10.1016/j.atmosenv.2006.11.020, 2007.

Draxler, R. R. and Rolph, G. D.: HYSPLIT (Hybrid Single-Particle Lagrangian Integrated Trajectory) Model access via NOAA ARL READY website at http://ready.arl.noaa.gov/HYSPLIT.php, last access: 1 March 2010, 2011.

Drewnick, F., Hings, S. S., Decarlo, P., Jayne, J. T., Gonin, M., Fuhrer, K., Weimer, S., Jimenez, J. L., Borrmann, K. L. D. S., and Worsnop, D. R.: A new time-of-flight aerosol mass spectrometer (TOF-AMS)-Instrument description and first field deployment, Aerosol Sci. Technol., 39, doi:10.1080/02786820500182040, 2005.

Dzepina, K., Volkamer, R. M., Madronich, S., Tulet, P., Ulbrich, I. M., Zhang, Q., Cappa, C. D., Ziemann, P. J., and Jimenez, J. L.: Evaluation of recently-proposed secondary organic aerosol models for a case study in Mexico City, Atmos. Chem. Phys., 9, 5681–5709, doi:10.5194/acp-9-5681-2009, 2009.

Fortin, T. J., Howard, B. J., Parrish, D. D., Goldan, P. D., Kuster, W. C., Atlas, E. L., and Harley, R. A.: Temporal changes in U.S. benzene emissions inferred from atmospheric measurements., Environ. Sci. Technol., 39, 1403–1408, 2005.

Fuller, G. W. and Green, D.: Evidence for increasing concentrations of primary PM10 in London, Atmos. Environ., 40, 6134-6145, doi:10.1016/j.atmosenv.2006.05.031, 2006.

Garland, R. M., Yang, H., Schmid, O., Rose, D., Nowak, A., Achtert, P., Wiedensohler, A., Takegawa, N., Kita, K., Miyazaki, Y., Kondo, Y., Hu, M., Shao, M., Zheng, L. M., Zhang, Y. H., Andreae, M. O., and Pöschl, U.: Aerosol optical properties in a rural environment near the mega-city Guangzhou, China: implications

for regional air pollution, radiative forcing and remote sensing, Atmos. Chem. Phys., 8, 5161–5186, doi:10.5194/acp-8-5161-2008, 2008.

de Gouw, J. A., Middlebrook, A. M., Warneke, C., Goldan, P. D., Kuster, W. C., Roberts, J. M., Fehsenfeld, F. C., Worsnop, D. R., Canagaratna, M. R., Pszenny, A. A. P., Keene, W. C., Marchewka, M., Bertman, S. B., and Bates, T. S.: Budget of organic carbon in a polluted atmosphere: Results from the New England Air Quality Study in 2002, J. Geophys. Res., 110, D16305, doi:10.1029/2004JD005623, 2005.

de Gouw, J. and Jimenez, J. L.: Organic aerosols in the Earth's atmosphere., Environ. Sci. Technol., 43, 7614–7618, doi:10.1021/es9006004, 2009.

Harley, R. A., Hannigan, M. P. and Cass, G. R.: Respeciation of organic gas emissions and the detection of excess unburned gasoline in the atmosphere, Environ. Sci. Technol., 26, 2395–2408, doi:10.1021/es00036a010, 1992.

Harrison, R. M., Jones, A. M. and Lawrence, R. G.: Major component composition of PM10 and $PM_{2.5}$ from roadside and urban background sites, Atmos. Environ., 38, 4531–4538, doi:10.1016/j.atmosenv.2004.05.022, 2004.

Haywood, J. M., Pelon, J., Formenti, P., Bharmal, N., Brooks, M., Capes, G., Chazette, P., Chou, C., Christopher, S., Coe, H., Cuesta, J., Derimian, Y., Desboeufs, K., Greed, G., Harrison, M., Heese, B., Highwood, E. J., Johnson, B., Mallet, M., Marticorena, B., Marsham, J., Milton, S., Myhre, G., Osborne, S. R., Parker, D. J., Rajot, J.-L., Schulz, M., Slingo, A., Tanré, D., and Tulet, P.: Overview of the Dust and Biomass-burning Experiment and African Monsoon Multidisciplinary Analysis Special Observing Period-0, J. Geophys. Res., 113, D00C17, doi:10.1029/2008JD010077, 2008a.

Haywood, J., Bush, M., Abel, S., Claxton, B., Coe, H., Crosier, J., Harrison, M., Macpherson, B., Naylor, M., and Osborne, S.: Prediction of visibility and aerosol within the operational Met Office Unified Model II?: Validation of model performance using observational data, Q. J. Roy. Meteorol. Soc., 134, 1817–1832, doi:10.1002/qj.275, 2008b.

Haywood, J., Francis, P., Osborne, S., Glew, M., Loeb, N., Highwood, E., Tanre, D., Myhre, G., Formenti, P., and Hirst, E.: Radiative properties and direct radiative effect of Saharan dust measured by the C-130 aircraft during SHADE: 1. Solar spectrum, J. Geophys. Res., 108, 1423–1447, doi:10.1029/2002JD002687, 2003.

Hewitt, C. N.: The atmospheric chemistry of sulphur and nitrogen in power station plumes, Atmos. Environ., 35, 1155–1170, doi:10.1016/S1352-2310(00)00463-5, 2001.

Highwood, E. J., Northway, M. J., McMeeking, G. R., Morgan, W. T., Liu, D., Osborne, S., Bower, K., Coe, H., Ryder, C., and Williams, P.: Scattering and absorption by aerosol during EUCAARI-LONGREX: can airborne measurements and models agree? Atmos. Chem. Phys. Discuss., 11, 18487-18525, doi:10.5194/acpd-11-18487-2011, 2011.

Hopkins, J. R., Boddy, R. K., Hamilton, J. F., Lee, J. D., Lewis, A. C., Purvis, R. M., and Watson, N. J.: An observational case study of ozone and precursors inflow to South East England during an anticyclone, J. Environ. Monitor., 8, 1195–202, doi:10.1039/b608062f, 2006.

Hopkins, J. R., Jones, C. E., and Lewis, A. C.: A dual channel gas chromatograph for atmospheric analysis of volatile organic compounds including oxygenated and monoterpene compounds, J. Environ. Monitor., 13, 2268-2276, doi:10.1039/c1em10050e, 2011.

Kleinman, L. I., Springston, S. R. Daum, P. H., Lee, Y.-N., Nunnermacker, L. J., Senum, G. I., Wang, J., Weinstein-Lloyd, J., Alexander, M. L., Hubbe, J., Ortega, J., Canagaratna, M. R., and Jayne, J.: The time evolution of aerosol composition over the Mexico City plateau, Atmos. Chem. Phys., 8, 1559–1575, doi:10.5194/acp-8-1559-2008, 2008.

Kleinman, L. I., Springston, S. R., Wang, J., Daum, P. H., Lee, Y.-N., Nunnermacker, L. J., Senum, G. I., Weinstein-Lloyd, J., Alexander, M. L., Hubbe, J., Ortega, J., Zaveri, R. A., Canagaratna, M. R., and Jayne, J.: The time evolution of aerosol size distribution over the Mexico City plateau, Atmos. Chem. Phys., 9, 4261-4278, doi:10.5194/acp-9-4261-2009, 2009.

Lack, D. A., Cappa, C. D., Covert, D. S., Baynard, T., Massoli, P., Sierau, B., Bates, T. S., Quinn, P. K., Lovejoy, E. R., Ravishankara, A. R., and Burkholder, J. B.: Bias in filter-based aerosol light absorption measurements due to organic aerosol loading: Evidence from laboratory measurements, Aerosol Sci. Technol., 42, 1033–1041, 2008.

Langford, B., Nemitz, E., House, E., Phillips, G. J., Famulari, D., Davison, B., Hopkins, J. R., Lewis, A. C., and Hewitt, C. N.: Fluxes and concentrations of volatile organic compounds above central London, UK, Atmos. Chem. Phys., 10, 627–645, doi:10.5194/acp-10-627-2010, 2010.

Lawrence, M. G., Butler, T. M., Steinkamp, J., Gurjar, B. R., and Lelieveld, J.: Regional pollution potentials of megacities and other major population centers, Atmos. Chem. Phys., 7, 3969–3987, doi:10.5194/acp-7-3969-2007, 2007.

McMeeking, G. R., Hamburger, T., Liu, D., Flynn, M., Morgan, W. T., Northway, M., Highwood, E. J., Krejci, R., Allan, J. D., Minikin, A., and Coe, H.: Black carbon measurements in the boundary layer over western and northern Europe, Atmos. Chem. Phys., 10, 9393–9414, doi:10.5194/acp-10-9393-2010, 2010.

McMeeking, G. R., Morgan, W. T., Flynn, M., Highwood, E. J., Turnbull, K., Haywood, J. and Coe, H.: Black carbon aerosol mixing state, organic aerosols and aerosol optical properties over the United Kingdom, Atmos. Chem. Phys., 11, 9037–9052, doi:10.5194/acp-11-9037-2011, 2011.

Menut, L., Vautard, R., Flamant, C., Abonnel, C., Beekmann, M., Chazette, P., Flamant, P. H., Gombert, D., Guédalia, D., Kley, D., Lefebvre, M. P., Lossec, B., Martin, D., Mégie, G., Perros, P., Sicard, M., and Toupance, G.: Measurements and modelling of atmospheric pollution over the Paris area: an overview of the ESQUIF Project, Ann. Geophys., 18, 1467–1481, doi:10.1007/s00585-000-1467-y, 2000.

Molina, L. T., Madronich, S., Gaffney, J. S., Apel, E., de Foy, B., Fast, J., Ferrare, R., Herndon, S., Jimenez, J. L., Lamb, B., Osornio-Vargas, A. R., Russell, P., Schauer, J. J., Stevens, P. S., Volkamer, R., and Zavala, M.: An overview of the MILAGRO 2006 Campaign: Mexico City emissions and their transport and transformation, Atmos. Chem. Phys., 10, 8697–8760, doi:10.5194/acp-10-8697-2010, 2010.

Molina, M. J. and Molina, L. T.: Megacities and atmospheric pollution., J. Air Waste Manage. Assoc., 54, 644–680, 2004.

Morgan, W. M., Allan, J. D., Bower, K. N., Capes, G., Crosier, J., Williams, P. I., and Coe, H.: Vertical distribution of sub-micron aerosol chemical composition from North-Western Europe and

the North-East Atlantic, Atmos. Chem. Phys., 9, 5389–5401, doi:10.5194/acp-9-5389-2009, 2009.

Morgan, W. T., Allan, J. D., Bower, K. N., Esselborn, M., Harris, B., Henzing, J. S., Highwood, E. J., Kiendler-Scharr, A., McMeeking, G. R., Mensah, A. A., Northway, M. J., Osborne, S., Williams, P. I., Krejci, R., and Coe, H.: Enhancement of the aerosol direct radiative effect by semi-volatile aerosol components: airborne measurements in North-Western Europe, Atmos. Chem. Phys., 10, 8151–8171, doi:10.5194/acp-10-8151-2010, 2010a.

Morgan, W. T., Allan, J. D., Bower, K. N., Highwood, E. J., Liu, D., McMeeking, G. R., Northway, M. J., Williams, P. I., Krejci, R. and Coe, H.: Airborne measurements of the spatial distribution of aerosol chemical composition across Europe and evolution of the organic fraction, Atmos. Chem. Phys., 10, 4065–4083, doi:10.5194/acp-10-4065-2010, 2010b.

Morino, Y., Kondo, Y., Takegawa, N., Miyazaki, Y., Kita, K., Komazaki, Y., Fukuda, M., Miyakawa, T., Moteki, N., and Worsnop, D. R.: Partitioning of HNO_3 and particulate nitrate over Tokyo: Effect of vertical mixing, J. Geophys. Res., D15215, doi:10.1029/2005JD006887, 2006.

Moteki, N. and Kondo, Y.: Effects of Mixing State on Black Carbon Measurements by Laser-Induced Incandescence, Aerosol Sci. Technol., 41, 398–417, doi:10.1080/02786820701199728, 2007.

Moteki, N., Kondo, Y., Miyazaki, Y., Takegawa, N., Komazaki, Y., Kurata, G., Shirai, T., Blake, D. R., Miyakawa, T., and Koike, M.: Evolution of mixing state of black carbon particles: Aircraft measurements over the western Pacific in March 2004, Geophys. Res. Lett., 34, L11803, doi:10.1029/2006GL028943, 2007.

Neuman, J. A., Nowak, J. B., Brock, C. A., Trainer, M., Fehsenfeld, F. C., Holloway, J. S., Hubler, G., Hudson, P. K., Murphy, D. M., Nicks, Jr., D. K., Orsini, D., Parrish, D. D., Ryerson, T. B., Sueper, D. T., Sullivan, A., and Weber, R., Variability in ammonium nitrate formation and nitric acid depletion with altitude and location over California, 4557, doi:10.1029/2003JD003616, 2003.

Parekh, P.: Ambient air quality of two metropolitan cities of Pakistan and its health implications, Atmos. Environ., 35, 5971–5978, doi:10.1016/S1352-2310(00)00569-0, 2001.

Parrish, D. D., Kuster, W. C., Shao, M., Yokouchi, Y., Kondo, Y., Goldan, P. D., de Gouw, J. A, Koike, M., and Shirai, T.: Comparison of air pollutant emissions among mega-cities, Atmos. Environ., 43, 6435–6441, doi:10.1016/j.atmosenv.2009.06.024, 2009.

Randriamiarisoa, H., Chazette, P., Couvert, P., Sanak, J., and Mégie, G.: Relative humidity impact on aerosol parameters in a Paris suburban area, Atmos. Chem. Phys., 6, 1389–1407, doi:10.5194/acp-6-1389-2006, 2006.

Raut, J.-C. and Chazette, P.: Retrieval of aerosol complex refractive index from a synergy between lidar, sunphotometer and in situ measurements during LISAIR experiment, Atmos. Chem. Phys., 7, 2797–2815, doi:10.5194/acp-7-2797-2007, 2007.

Raut, J.-C. and Chazette, P.: Assessment of vertically-resolved PM10 from mobile lidar observations, Atmos. Chem. Phys., 9, 8617–8638, doi:10.5194/acp-9-8617-2009, 2009.

Royer, P., Chazette, P., Lardier, M., and Sauvage, L.: Aerosol content survey by mini N2-Raman lidar: Application to local and long-range transport aerosols, Environ., 45, 7487–7495, doi:10.1016/j.atmosenv.2010.11.001, 2011a.

Royer, P., Chazette, P., Sartelet, K., Zhang, Q. J., Beekmann, M., and Raut, J.-C.: Comparison of lidar-derived PM_{10} with regional modeling and ground-based observations in the frame of MEGAPOLI experiment, Atmos. Chem. Phys., 11, 10705–10726, doi:10.5194/acp-11-10705-2011, 2011b.

Ryder, C. L. and Toumi, R.: An urban solar flux island: Measurements from London, Atmos. Environ., 45, 3414–3423, doi:10.1016/j.atmosenv.2011.03.045, 2011.

Schwarz, J. P., Gao, R. S., Fahey, D. W., Thomson, D. S., Watts, L. A., Wilson, J. C., Reeves, J. M., Darbeheshti, M., Baumgardner, D. G., Kok, G. L., Chung, S. H., Schulz, M., Hendricks, J., Lauer, A., Kärcher, B., Slowik, J. G., Rosenlof, K. H., Thompson, T. L., Langford, A. O., Loewenstein, M., and Aikin, K. C.: Single-particle measurements of midlatitude black carbon and light-scattering aerosols from the boundary layer to the lower stratosphere, J. Geophys. Res., 111, D16207, doi:10.1029/2006JD007076, 2006.

Schwarz, J. P., Spackman, J. R., Fahey, D. W., Gao, R. S., Lohmann, U., Stier, P., Watts, L. A., Thomson, D. S., Lack, D. A., Pfister, L., Mahoney, M. J., Baumgardner, D., Wilson, J. C., and Reeves, J. M.: Coatings and their enhancement of black carbon light absorption in the tropical atmosphere, J. Geophys. Res., 113, D03203, doi:10.1029/2007JD009042, 2008.

Seila, R. L., Lonneman, W. A., and Meeks, S. A.: Determination of C2 to C12 ambient air hydrocarbons in 39 U.S. cities, from 1984 through 1986, US Environmental Protection Agency, Washington, DC, USA, 1989.

Shinozuka, Y., Clarke, A. D., Howell, S. G., Kapustin, V. N., McNaughton, C. S., Zhou, J., and Anderson, B. E.: Aircraft profiles of aerosol microphysics and optical properties over North America: Aerosol optical depth and its association with $PM_{2.5}$ and water uptake, J. Geophys. Res., 112, D12S20, doi:10.1029/2006JD007918, 2007.

Spackman, J. R., Schwarz, J. P., Gao, R. S., Watts, L. A., Thomson, D. S., Fahey, D. W., Holloway, J. S., de Gouw, J. A., Trainer, M., and Ryerson, T. B.: Empirical correlations between black carbon aerosol and carbon monoxide in the lower and middle troposphere, Geophys. Res. Lett., 35, L19816, doi:10.1029/2008GL035237, 2008.

Subramanian, R., Kok, G. L., Baumgardner, D., Clarke, A., Shinozuka, Y., Campos, T. L., Heizer, C. G., Stephens, B. B., de Foy, B., Voss, P. B., and Zaveri, R. A.: Black carbon over Mexico: the effect of atmospheric transport on mixing state, mass absorption cross-section, and BC/CO ratios, Atmos. Chem. Phys., 10, 219–237, doi:10.5194/acp-10-219-2010, 2010.

Svenningsson, B., Rissler, J., Swietlicki, E., Mircea, M., Bilde, M., Facchini, M. C., Decesari, S., Fuzzi, S., Zhou, J., Mønster, J., and Rosenørn, T: Hygroscopic growth and critical supersaturations for mixed aerosol particles of inorganic and organic compounds of atmospheric relevance, Atmos. Chem. Phys., 6, 1937–1952, doi:10.5194/acp-6-1937-2006, 2006.

Visschedijk, A., Zandveld, P., and Van Der Gon, H. D.: A high resolution gridded European emission database for the EU integrated project GEMS, Apeldoorn, The Netherlands, 2007.

von Schneidemesser, E., Monks, P. S., and Plass-Duelmer, C.: Global comparison of VOC and CO observations in urban areas, Atmos. Environ., 44, 5053–5064, 2010.

von Schneidemesser, E., Monks, P. S., Gros, V., Gauduin, J., and Sanchez, O.: How important is biogenic isoprene in an urban

environment? A study in London and Paris, Geophys. Res. Lett., 38, L19804, doi:10.1029/2011GL048647, 2011.

Warneke, C., McKeen, S. a, de Gouw, J. a, Goldan, P. D., Kuster, W. C., Holloway, J. S., Williams, E. J., Lerner, B. M., Parrish, D. D., Trainer, M., Fehsenfeld, F. C., Kato, S., Atlas, E. L., Baker, A., and Blake, D. R.: Determination of urban volatile organic compound emission ratios and comparison with an emissions database, J. Geophys. Res., 112, D10S47, doi:10.1029/2006JD007930, 2007.

Yokelson, R. J., Urbanski, S. P., Atlas, E. L., Toohey, D. W., Alvarado, E. C., Crounse, J. D., Wennberg, P. O., Fisher, M. E., Wold, C. E., Campos, T. L., Adachi, K., Buseck, P. R., and Hao, W. M.: Emissions from forest fires near Mexico City, Atmos. Chem. Phys., 7, 5569–5584, doi:10.5194/acp-7-5569-2007, 2007.